T.&A.M. Report No. 480

CREEP CONSTITUTIVE EQUATIONS FOR DAMAGED MATERIALS

by

A.C.F. Cocks* and F. A. Leckie
Department of Theoretical and Applied Mechanics
University of Illinois at Urbana-Champaign

March 1986

*Present address: Department of Engineering, Leicester University, Leicester, England

Nomenclature

ε_{ij}^{e}, ε_{ij}^{p}, ε_{ij}^{T}	Elastic, plastic and total strains
$E_{ij}^{\alpha e}$, $E_{ij}^{\alpha p}$, E_{ij}^{α}	Mean elastic, plastic and total strains experienced by a grain-boundary element of material with outward normals $\underline{n}_1^{\alpha}$ and $\underline{n}_2^{\alpha}$.
E_{ij}^{e}, E_{ij}^{p}, E_{ij}	Mean elastic, plastic and total strains of macroscopic element of material
σ_{ij}	Stress
Σ_{ij}^{α}	Mean stress in grain-boundary element of material
Σ_{ij}	Stress applied to a macroscopic element of material
$\hat{\sigma}_{ij}$	Equilibrium stress field resulting from elastic analysis
ρ_{ij}	Residual stress field
Σ_c, Σ_h, Σ_n	Thermodynamic stresses associated with different internal state variables.
Σ_I, Σ_{II}, Σ_{III}	Principal applied stresses
Σ_n^{α}	Stress normal to a grain boundary
$C_{ijk\ell}$, $D_{ijk\ell}$	Elastic compliance and stiffness matrices
$\dot{\varepsilon}_o$, σ_o, n	Constants in creep law of eqn. (3.1)
ϕ	Helmholtz free energy
α_k	Internal displacement variables
s_k	Thermodynamic force associated with α_k
η_g, η_c	Internal state variable used in the analysis of strain-softening
F_k, F_v	Thermodynamic driving forces for irreversible processes
V	Volume

V_α	Volume of material element with outward normals $\underline{n}_1^\alpha$ and $\underline{n}_2^\alpha$
A_α	Area of grain boundary
v_α	Volume fraction of grain-boundary elements of volume V_α
ρ_α	Measure of the density of grain-boundary cracks
r_h	Void radius
r_c	Critical void radius required for nucleation
2ℓ	Void spacing
n	Number of voids in grain-boundary element
n_s	Number of potential nucleation sites
$\underline{n}_1^\alpha$, $\underline{n}_2^\alpha$	Outward normals to a grain boundary
Φ	Strain-rate and damage-rate potential
Ω, Δ	Temperature dependent material properties
ω	Scalar measure of damage
ν	Creep damage exponent
λ	Creep damage tolerance
ε_f	Strain to failure
t_f	Time to failure
t_f^i	Time to initiate failure in a structure
$\chi(\sigma_{ij})$	Convex function of stress appearing in damage growth rate equation
χ_c	Value of $\chi(\sigma_{ij})$ at yield for a perfectly plastic material
μ	Plastic multiplier

1. Introduction

Constitutive equations used by the engineer to describe the plastic behavior of materials have largely been developed intuitively, the main concern being that the equations should describe the material macroscopic properties while retaining sufficient simplicity to allow convenient structural analysis. A common and convenient approach is to describe the material behavior in terms of internal state variables, and to assume the existence of a scalar convex potential from which the strain-rate and rate of change of internal state variables can be derived. This allows the proof of uniqueness and the development of bounding theorems.

This intuitive approach is consistent with a thermodynamic description expressed in terms of internal state variables which are obtained from an understanding of the microscopic mechanisms that lead to plastic flow. Rice [1] proved the existence of a potential from the fact that plastic straining is due to the motion of dislocations through the material. Simple modeling of the dislocation mechanisms further permits the identification of a number of scalar and second order tensor state variables [2,3] (which relate to the shear yield strength of a family of slip systems and the residual stress field developed during plastic straining). The evolution of the state variables can be found from the potential which can be shown to be convex. The advantage of such an approach is that it gives a framework for the development of more complex constitutive models and, perhaps more importantly, an indication of those loading conditions for which a single state variable model adequately describes the material and structural response.

At high temperatures a material subjected to a constant stress can creep and eventually fail due to the growth of internal damage. The engineering approach is again largely intuitive. State variables which measure the amount

of damage are introduced into the constitutive equations. Additional rules are developed for the evolution of the state variables with time and failure occurs when one of the variables reaches a critical value. This approach has proven successful for situations of constant load and in situations involving moderate levels of cyclic loading.

In a recent paper Ashby and Dyson [4] have examined all the presently known mechanisms of failure in creeping materials. A list of these mechanisms is given in Table 1. They are divided into three groups: geometric, environmental and bulk mechanisms. Geometric instabilities can be explained using constitutive equations developed for the bulk mechanisms taking into account changes in geometry resulting from large plastic deformation. Premature failure can occur in aggressive environments due to the loss in load carrying capacity of a surface layer which increases in thickness with time. This load is shed onto the remainder of the body which deforms and becomes damaged by one of the bulk mechanisms. Central to the understanding of all these failures is the understanding of the bulk mechanisms of damage to which this paper is devoted.

The object of the present paper is to combine this knowledge of the microscopic mechanisms with experimental observations to obtain constitutive equations for damaged materials. Initially we concentrate entirely on the mechanisms described above and obtain a general structure for the constitutive equations. This gives a framework for the development of constitutive equations for particular materials. In the present paper we attempt to do this for the copper and an aluminum alloy tested by Leckie and Hayhurst [5,6]. Throughout the development of this paper it should be remembered that any theoretical constitutive equations should be verifiable experimentally. This means that these equations should only contain a limited number of

experimentally obtained quantities and state variables.

The general structure for the constitutive equations is obtained by following the approach of Rice [1] in identifying a number of intenal state variables. The state of the material is then described in terms of its Helmholtz free energy from which we derive the thermodynamic forces associated with each state variable. When the rate of increase of the internal variables are only functions of their associated forces and the present state of the material it is possible to prove the existence of a scalar potential from which the inelastic strain-rate and rate of increase of the state variables are derivable. We find this to be true for situations where the damage is in the form of voids, but, as we shall see in section 7, this is not necessarily the most appropriate form for the constitutive laws. A situation for which it is convenient to express the material response in terms of a single potential occurs in precipitate hardened materials when the damage is in the form of dislocation networks which grow around the precipitate particles.

The thermodynamics is developed in section 2. In section 3 we examine each mechanism of void growth and in section 4 we briefly discuss the process of void nucleation. The analyses of these sections result in constitutive equations with a large number of state variables. This can be partially overcome by formulating the problem in terms of the distribution of damage in the material. We do this in section 5 following a method proposed by Onat and Leckie [7]. In section 6 we examine the strain softening mechanism proposed by Ashby and Dyson [4] and Henderson and McLean [8] which has recently been analysed by Cocks [9].

Sections 2 to 6 are concerned primarily with the basic structure of the constitutive equations. When the damage is in the form of voids we need to know the distribution of these voids within the body before being able to

obtain the exact constitutive laws. Constitutive equations are presented in section 7 for two simple distributions of voids which result in zero and full constraint as defined by Dyson [10]. In section 9 we analyze the experimental data available to us to make decisions on the structure of the material laws. In general the amount of information available is quite limited and we must be content with sets of equations which contain a limited number of state variables. The type and physical nature of the state variables that prove appropriate in a given situation can change as the type of loading (monotonic, non-proportional, cyclic) is changed.

The remainder of the paper is devoted to the application of the material models to structural problems. It is found that when the rate of increase of damage is mathematically separable in expressions for stress and of damage that it is possible to obtain upper bounds to the life of a component.

2. Thermodynamic Formalism

In this section we present a general thermodynamic description of material behavior in terms of internal state variables which are either a measure of the present dislocation structure or of the distribution and size of voids within the material. We identify the conditions under which it is possible to derive a scalar potential from which the strain-rate and rate of change of internal state variables can be derived. In later sections it is shown that the proposed mechanisms for void nucleation and growth as well as that for strain softening satisfy these conditions. The approach described here follows that used by Rice [1].

At a given instant in time we can define the state of the material using the Helmholtz free energy, which is expressed in terms of the position of any dislocations, the size, shape and distribution of any voids and the applied

load. This equation of state can only be obtained by postulating a reversible process by which the present state could be reached. The free energy is calculated by following this path to the present state. There may be a large number of such reversible paths, and the one chosen need not parallel the actual path that is followed during the irreversible process. For the situations considered in this paper the reversible paths followed are purely conceptual and cannot be followed in practice. When we define the state of the material in terms of the present dislocation structure we introduce the dislocations into the material by a series of cutting, displacing and resealing operations [1,2,3]. When voids grow in the material by a diffusion controlled process we form the voids by scooping material out and spreading this material evenly along the grain-boundary. In each case the contribution to the free energy can be written as

$$\psi = f(\alpha_k)\, V \tag{2.1}$$

where each α_k represents the position of a dislocation or the volume fraction of voids within an element of material, and is either a scalar vector or second order tensor, and V is the volume of the element of material. The total free energy can be found by loading the material elastically to the present stress:

$$\psi = (\tfrac{1}{2}\, C_{ijk\ell}\, \varepsilon^e_{k\ell}\, \varepsilon^e_{ij} + f(\alpha_k))V \tag{2.2}$$

where $C_{ijk\ell}$ is the elastic stiffness tensor which may be a function of the α_k's, and $\varepsilon^e_{k\ell}$ is the elastic strain resulting from the application of the applied stress σ_{ij}. Where α_k represents the dislocation structure, the uncoupling of the contributions to the free energy from ε^e_{ij} and α_k follows from the fact that the stress field which results from the presence of the

dislocations is a residual stress field.

Here we have expressed the free energy in terms of the elastic strain ε^e_{ij} rather than the total strain ε^T_{ij} and the plastic strain ε^P_{ij}. Use of ε^T_{ij} and ε^P_{ij} implies that the history of loading is known and, since ε^P_{ij} is a function of α_i, that the final state is uniquely related to this history, whereas in practice a given dislocation distribution can be obtained by following a large number of different reversible and irreversible paths. Also we can follow two histories of loadings which give the same plastic strain, but completely different dislocation structures. For example a material which is loaded monotonically to a uniaxial strain ε could have a lower yield stress and a completely different dislocation structure to a sample which is cycled between ε and $-\varepsilon$ for a number of cycles.

The thermodynamic forces associated with the state variables ε^e_{ij} and α_i can be found by differentiating eqn (2.2):

$$\dot{\psi} = (\sigma_{ij}\ \dot{\varepsilon}^e_{ij} + s_k \dot{\alpha}_k)V \tag{2.3}$$

where

$$\sigma_{ij}\ V = \frac{\partial \psi}{\partial \varepsilon^e_{ij}}$$

and

$$s_i\ V = \frac{\partial \psi}{\partial \alpha_k} \tag{2.4}$$

where s_k has the same tensorial nature as α_k. Here, and throughout this paper, a repeating index implies summation over all the internal variables.

We now accept the Clausius-Duhem inequality as the proper statement of the second law of thermodynamics for irreversible processes:

$$V \frac{dS}{dt} + \frac{\partial}{\partial x_i}\left[\frac{q_i}{T}\right] = \dot{\theta} \geqslant 0 \tag{2.5}$$

where S is the entropy per unit volume, q_i is the rate of heat flux out of an element of material, T is the absolute temperature, x_i is distance from some origin and $\dot{\theta}$ is the rate of entropy production. For isothermal processes eqn (2.5) becomes, after making the usual manipulations [1],

$$\sigma_{ij} \dot{\varepsilon}^T_{ij} V - \dot{\psi} \geq 0 \tag{2.6}$$

Substituting eqn (2.3) into this equation gives

$$\sigma_{ij} \dot{\varepsilon}^P_{ij} - s_k \dot{\alpha}_k \geq 0 \tag{2.7}$$

where $\dot{\varepsilon}^P_{ij} = \dot{\varepsilon}^T_{ij} - \dot{\varepsilon}^e_{ij}$ is the inelastic strain rate. This strain results from the motion of dislocations through the material or from the growth of voids, so that

$$\dot{\varepsilon}^P_{ij} = g_k \dot{\alpha}_k \tag{2.8}$$

where g_k is a second-order tensor if α_k is a scalar; third order tensor if α_k is a vector; a fourth order tensor if α_k is a second order tensor. Combining eqns (2.7) and (2.8) gives

$$(\sigma_{ij} g_k - s_k) \dot{\alpha}_k \geq 0 \tag{2.9}$$

or

$$F_k \dot{\alpha}_k \geq 0$$

where

$$F_k = (\sigma_{ij} g_k - s_k)$$

is the thermodynamic driving force for the process.

To proceed further we need expressions for the $\dot{\alpha}_k$'s in terms of the state variables and their affinities. For each damaging mechanism examined in the following sections we find that

$$\dot{\alpha}_k = \dot{\alpha}_k \ (F_k, \ \alpha_k) \tag{2.10}$$

i.e., $\dot{\alpha}_k$ is only a function of the Affinity associated with it, F_k , and the present state of the material. In such situations Rice [1] has shown that it is possible to find a scalar potential from which the inelastic strain-rate can be derived. We repeat that proof here and further show that in addition the rate of change of the internal state variables are derivable from the same potential.

If we multiply both sides of eqn (2.8) by $d\sigma_{ij}$ we find

$$\dot{\varepsilon}^P_{ij} \ d\sigma_{ij} = g_k \ \dot{\alpha}_k \ d\sigma_{ij} \tag{2.11}$$

From eqn (2.9) we note

$$\frac{\partial F_k}{\partial \sigma_{ij}} = g_k \tag{2.12}$$

Substituting this and eqn (2.10) into eqn (2.11) gives

$$\dot{\varepsilon}^P_{ij} \ d\sigma_{ij} = \dot{\alpha}_k(F_k, \ \alpha_k) \ \frac{\partial F_k}{\partial \sigma_{ij}} \ d\sigma_{ij}$$

At a given instant in time we know the state variables α_k. Treating these as constants in the above expression gives

$$\dot{\varepsilon}^P_{ij} \ d\sigma_{ij} = \dot{\alpha}_k(F_k, \ \alpha_k) \ dF_k = d\Phi \tag{2.13}$$

The r.h.s. of eqn (2.13) is now an exact differential:

$$\int_0^{F_k} \dot{\alpha}_k(F_k, \ \alpha_k) \ dF_k = \Phi \tag{2.14}$$

and

$$\dot{\varepsilon}^P_{ij} = \frac{\partial \Phi}{\partial \sigma_{ij}} \tag{2.15}$$

This is the result originally found by Rice [1]. Further, eqn (2.13) gives

$$\dot{\alpha}_k = \frac{\partial \Phi}{\partial F_k} = - \frac{\partial \Phi}{\partial s_k} \tag{2.16}$$

We make use of eqns (2.15) and (2.16) in the following sections where we analyse each of the bulk damaging processes.

The results obtained in this section so far are central to the developments in the remainder of this paper. Because of the importance of these results we summarize them briefly below:

The internal structure of the material is described in terms of a number of internal state variables α_k, such that the Helmholtz free energy takes the form

$$\psi = \psi(\underset{\sim}{\varepsilon}^e, \alpha_k)$$

The thermodynamic forces are then

$$\sigma_{ij}\, V = \frac{\partial \psi}{\partial \varepsilon_{ij}} \; ; \quad s_k V = \frac{\partial \psi}{\partial \alpha_k}$$

If eqn. (2.10) is satisfied the inelastic strain-rate and rate of increase of the internal variables can be derived from a potential Φ:

$$\dot{\varepsilon}^p_{ij} = \frac{\partial \Phi}{\partial \sigma_{ij}} \; ; \quad \dot{\alpha}_k = - \frac{\partial \Phi}{\partial s_k}$$

Next we consider a composite material, for which equations (2.15) and (2.16) hold in each element. This analysis allows us to piece together a number of microscopic elements to give the overall response of a macroscopic element of material. For simplicity we will also assume that there is only one state variable associated with each element. At a given instant the total strain rate in each element for a constant remote stress Σ_{ij} is

$$\dot{\varepsilon}^T_{ij} = \dot{\varepsilon}^e_{ij} + \dot{\varepsilon}^P_{ij}$$

which is compatible with the remote strain-rate field $\dot{E}^P_{ij}$. If $d\sigma_{ij}$ is the increment of stress in each element for an increment of remote stress $d\Sigma_{ij}$ when the material responds elastically, application of the principle of virtual work gives

$$\dot{E}^P_{ij}\ d\Sigma_{ij}\ V = \sum_k (\dot{\varepsilon}^e_{ij} + \dot{\varepsilon}^P_{ij})\ d\sigma_{ij}\ V_k \tag{2.17}$$

where $\dot{E}^P_{ij}$ is the remote inelastic strain-rate, V is the total volume of the composite and V_k is the volume of the kth element. Rearranging eqn (2.17) gives

$$\dot{E}^P_{ij}\ d\Sigma_{ij}\ V = \sum_k \dot{\varepsilon}^e_{ij}\ d\sigma_{ij}\ V_k + \sum_k \dot{\varepsilon}^P_{ij}\ d\sigma_{ij}\ V_k \tag{2.18}$$

The elastic strain-rate $\dot{\varepsilon}^e_{ij}$ gives rise to a changing residual stress field $\dot{\rho}_{ij}$, and associated with the stress field $d\sigma_{ij}$ is an elastic strain field $d\varepsilon^e_{ij}$. Eqn. (2.18) then becomes, after making use of eqn. (2.15),

$$\dot{E}^P_{ij}\ d\Sigma_{ij}\ V = \sum_k D_{ijk\ell}\ \dot{\rho}_{k\ell}\ d\sigma_{ij}\ V_k + \sum_k \frac{\partial \Phi^k}{\partial \sigma_{ij}}\ d\sigma_{ij}\ V_k$$

$$= \Sigma_k\ D_{k\ell ij}\ d\sigma_{ij}\ \dot{\rho}_{k\ell} + \Sigma_k \frac{\partial \Phi^k}{\partial \sigma_{ij}}\ d\sigma_{ij}\ V_k \tag{2.19}$$

where $D_{ijk\ell}$ is the elastic compliance tensor, and Φ^k is the potential for the kth element:

$$\Phi^k = \Phi^k\ (\sigma_{ij},\ s_k,\ \alpha_k)$$

The increment of Φ^k for constant α_k is then

$$d\Phi^k = \frac{\partial \Phi^k}{\partial \sigma_{ij}}\ d\sigma_{ij} + \frac{\partial \Phi^k}{\partial s_k}\ ds_k \tag{2.20}$$

Substituting eqn (2.20) into eqn (2.19) gives

$$\dot{E}^P_{ij}\, d\Sigma_{ij}\, V = \sum_k \dot{\rho}_{ij}\, d\varepsilon^e_{ij}\, V_k + \sum_k d\Phi^k\, V_k + \sum_k \frac{\partial \Phi^k}{\partial s_k}\, ds_k \qquad (2.21)$$

Since $\dot{\rho}_{ij}$ is a residual stress field and $d\varepsilon^e_{ij}$ a compatible strain field the first term on the r.h.s. of eqn (2.21) is zero. Rearranging eqn (2.20) and noting eqn (2.16) gives

$$\dot{E}^P_{ij}\, d\Sigma_{ij}\, V - \sum_k \dot{\alpha}_k\, ds_k\, V_k = \sum_k d\Phi_k\, V_k = d\Phi\, V$$

Therefore

$$E^P_{ij} = \frac{\partial \Phi}{\partial \Sigma_{ij}}$$

and

$$\dot{\alpha}_k = - v_k \frac{\partial \Phi}{\partial s_k} \qquad (2.22)$$

where

$$v_k = V_k / V$$

Equation (2.22) demonstrates that for the composite system it is possible to obtain a single macroscopic potential, which is the volume average of the microscopic potentials, from which the strain-rate and rate of change of internal variables can be derived.

The macroscopic potential Φ contains information about the residual stress field, ρ_{ij}, within the material which results from the non-uniform accumulation of plastic strain. Cocks and Ponter [3] demonstrate that the rate of change of the residual stresses are also derivable from Φ. We do not include these expressions here so as not to cloud the general results of this paper. Specific forms for the function Φ are given in sections 6 to 8. The residual stress fields in these expressions remain constant as the damage increases, so that the evolution laws for the residual stress field are not

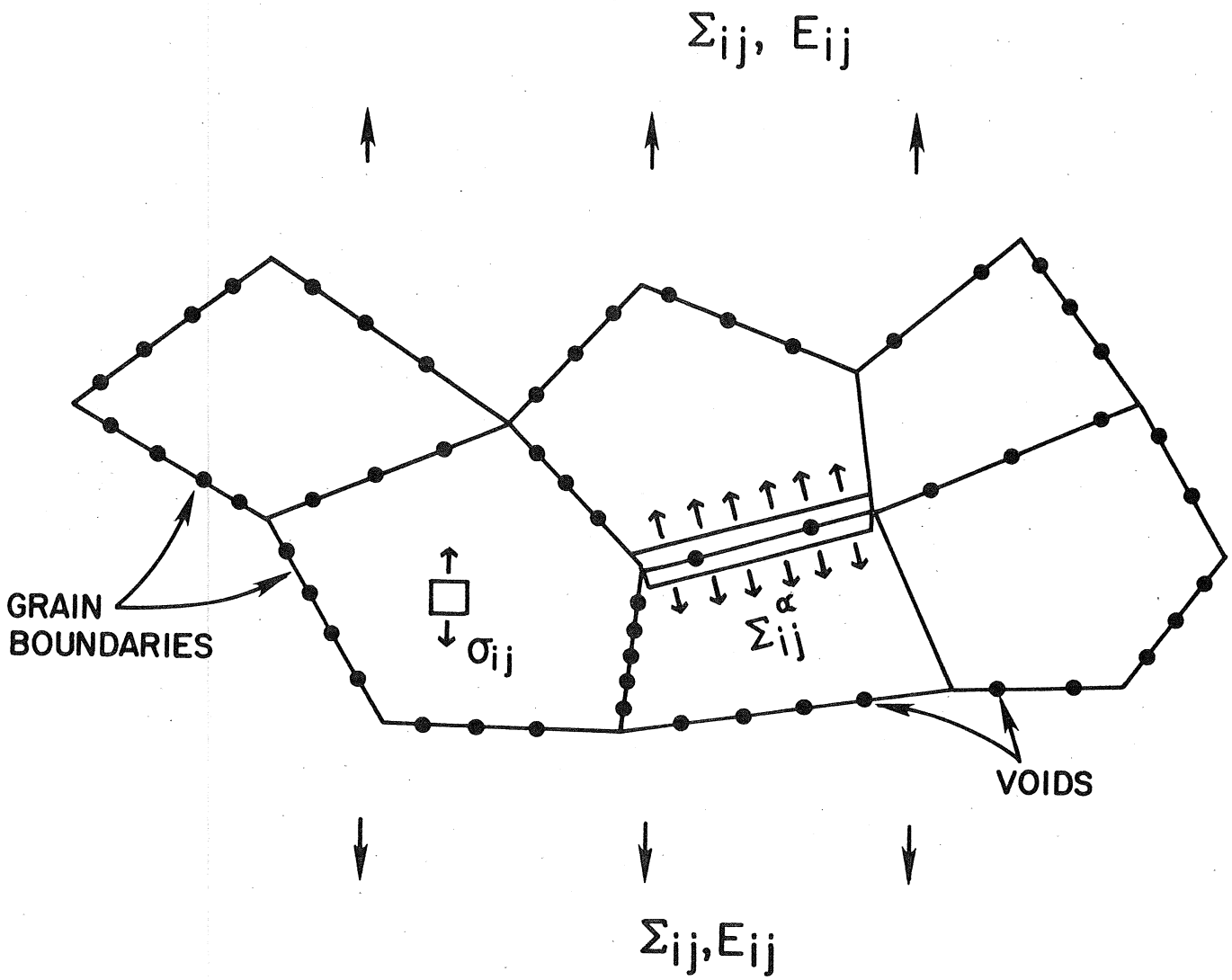

Fig. 1. An element of material containing a number of cavitated grain boundaries subjected to a stress Σ_{ij}.

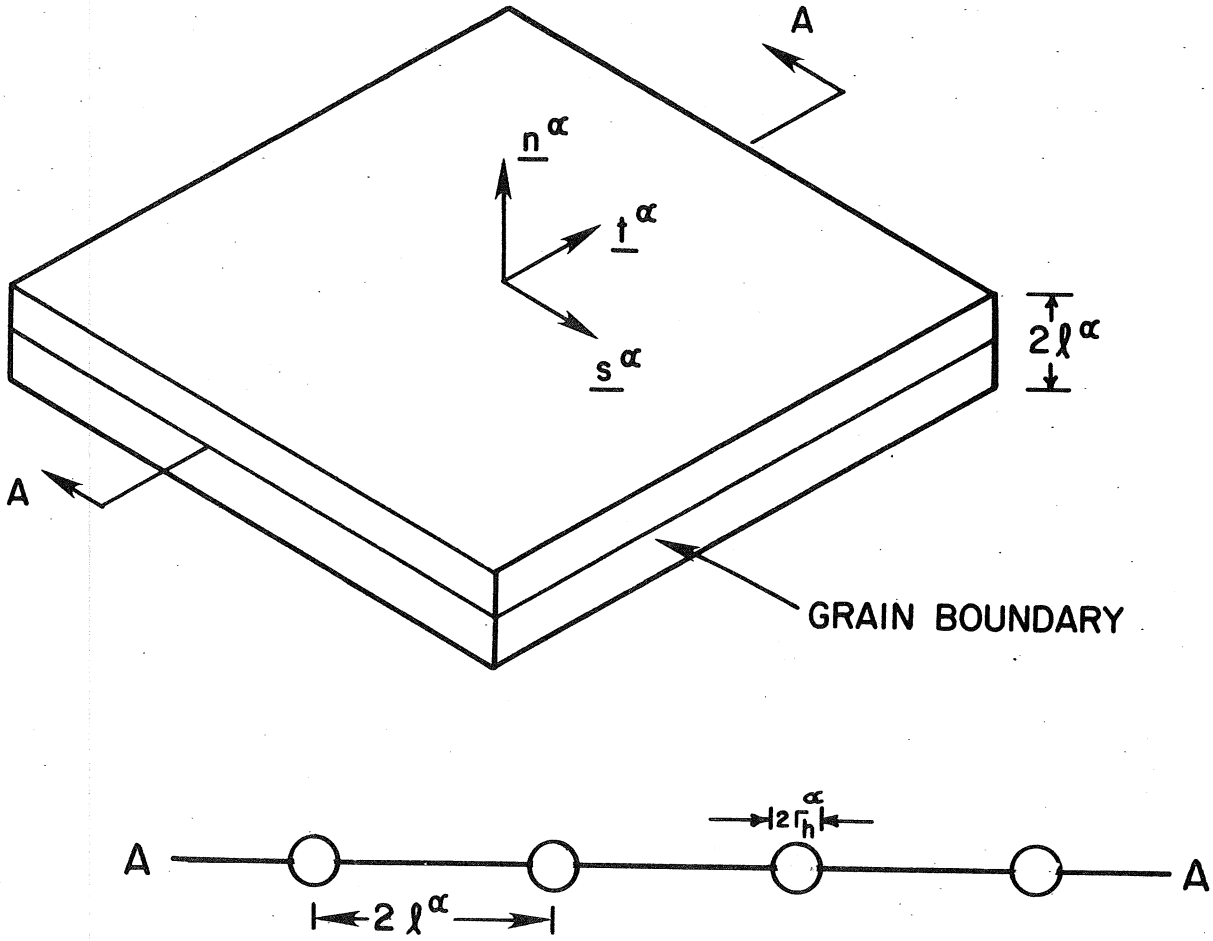

Fig. 2. A typical grain-boundary slab of material in Fig. 2, which contains voids of radius r_h^α spaced a distance $2\ell^\alpha$ apart.

required.

3. Mechanisms of Void Growth

As the material creeps, voids can either grow within the grains or on the grain boundaries. In structural situations, when the design life of a component is long, the most common mode of failure involves the growth of intergranular voids. The general situation we consider in this section is shown in Fig. 1, where we assume that the number and spacing of the voids remains fixed during the life. The influence of the nucleation of additional voids is examined in the next section.

The analysis of this problem is facilitated by isolating a volume of material surrounding a grain boundary and examining the response of this element. The behavior of the entire material is then found by combining all of the elements to form a composite system. A typical grain-boundary element is shown in Fig. 2. We characterize the position of this boundary in terms of its outward normals $\underline{n}_1^\alpha$ and $\underline{n}_2^\alpha$.

The voids within an element of material can grow by one of a number of mechanisms: power law creep; grain-boundary diffusion; surface diffusion; or by a coupling of any two or all three of these mechanisms. Cocks and Ashby [12] have shown however that the materials response can be adequately described if it is assumed that the dominant mechanism of the three simple mechanisms operates alone. These mechanisms are shown in Fig. 3 and we consider each in turn in the following sub-sections. The strain resulting from the growth of these voids is accommodated in the rest of the material by deformation due to power-law creep and by grain-boundary sliding. We examine grain-boundary sliding separately in section 3.4 and the overall response of a macroscopic element in section 3.5.

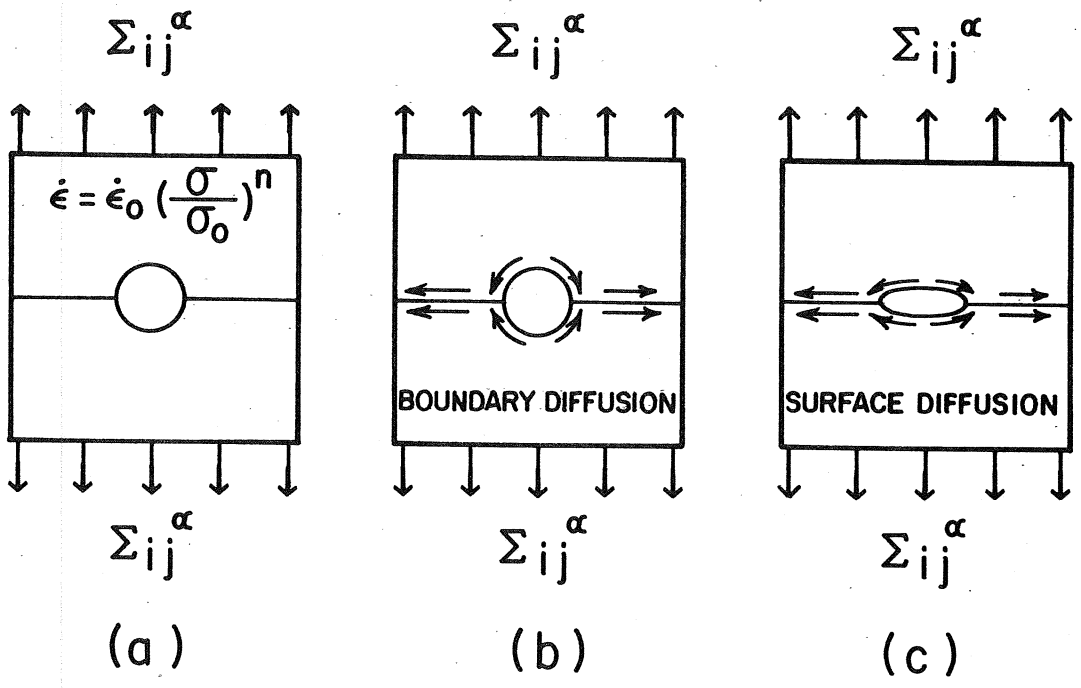

Fig. 3. The rate of growth of the voids can be controlled by: (a) power-law creep, (b) grain-boundary diffusion, or (c) surface diffusion.

3.1 Void Growth by Power-Law Creep

Cocks and Ponter [2] have analyzed creep deformation by power-law creep for a void-free material using the thermodynamic approach described in the last section. For constant or slowly changing stresses it is possible to define a steady state potential such that

$$\dot{\varepsilon}_{ij} = \frac{\partial \phi}{\partial \sigma_{ij}} \tag{3.1}$$

It is often assumed that

$$\phi = \frac{\sigma_o \dot{\varepsilon}_o}{(n+1)} \left(\frac{\sigma_e}{\sigma_o}\right)^{n+1}$$

where σ_o, $\dot{\varepsilon}_o$ and n are material constants and σ_e is an effective stress. We use equation (3.1) as the starting point for the analysis of this section.

The state of the material can be described in terms of the volume fraction of voids, f_v^α, which it contains. If it is assumed that all the voids are the same size and are uniformly spaced along the boundary then we can further isolate an element of material of volume $\overline{V}^\alpha$ which contains a single void, Fig. 4, and assume that it experience the stress applied to the grain-boundary element of Fig. 1. Analyses of this type give the mean strain-rate, $\dot{E}_{ij}^\alpha$, of the grain-boundary element. This strain-rate can be obtained from the following energy balance.

$$\Sigma_{ij}^\alpha \dot{E}_{ij}^\alpha \overline{V}^\alpha - \gamma_s \dot{A}_s = \int_{\overline{V}^\alpha} \sigma_{ij} \dot{\varepsilon}_{ij} \, dV \tag{3.2}$$

The second term on the l.h.s. arises from the increase in surface energy as the surface area A_s of the void increases.

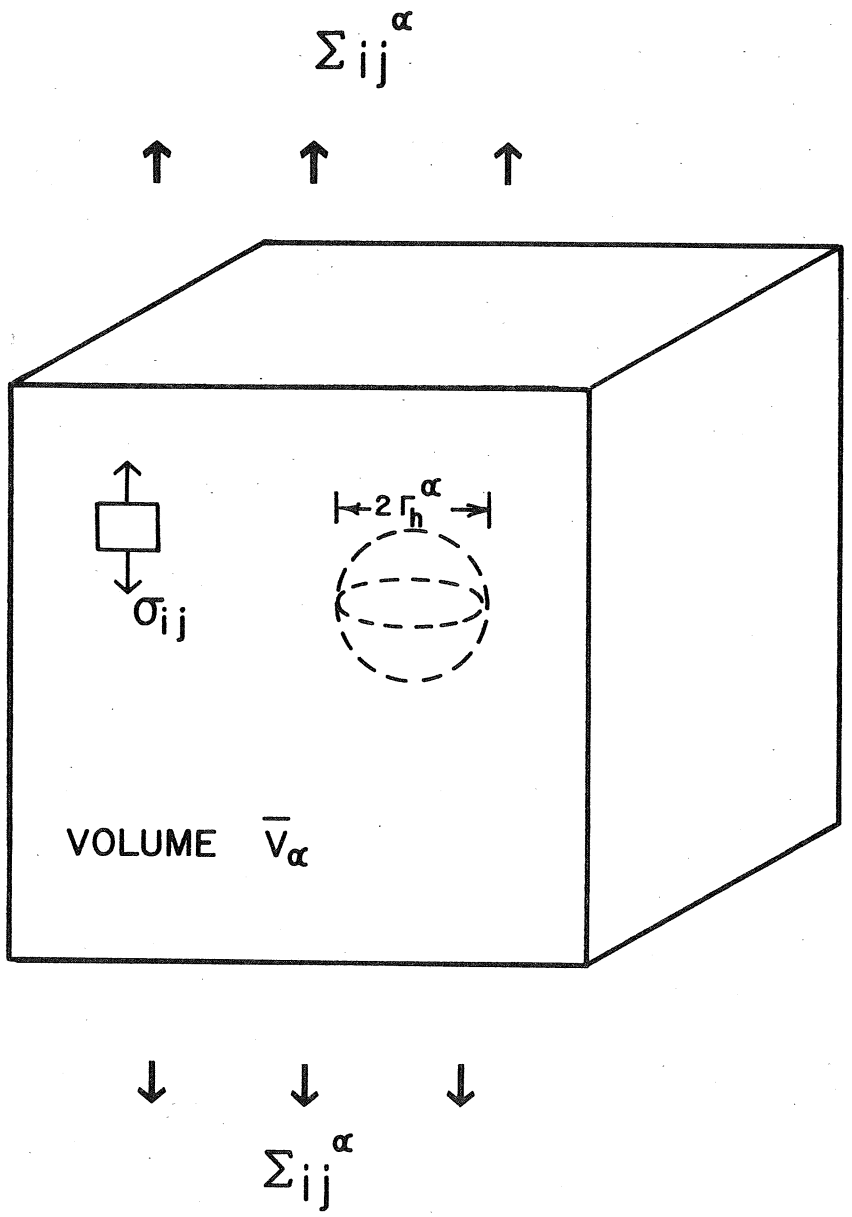

Fig. 4. A void of radius Γ_h embedded in an element of material of volume V, which is subjected to a stress Σ_{ij}.

Now

$$A_s = 4 \pi r_h^2$$

and the volume of the void

$$V_h = \frac{4}{3} \pi r_h^3$$

Therefore
$$\dot{A}_s = \frac{2 \dot{V}_h}{r_h} = \frac{2 \dot{f}_v^\alpha}{r_h} \overline{V}^\alpha \tag{3.3}$$

where $f_v^\alpha = \frac{V_h}{\overline{V}^\alpha}$ is the volume fraction of voids. Substituting eqn. (3.3) into eqn. (3.2) gives

$$\Sigma_{ij}^\alpha \dot{E}_{ij}^\alpha - \Sigma_c^\alpha \dot{f}_v^\alpha = \frac{1}{\overline{V}^\alpha} \int_{\overline{V}^\alpha} \sigma_{ij} \dot{\varepsilon}_{ij} \, dV \tag{3.4}$$

where $\Sigma_c = \frac{2\gamma_s}{r_h}$. Σ_c is simply the surface tension and eqn. (3.4) is a statement of virtual work, with Σ_c treated as an applied surface traction.

The microscopic stress σ_{ij} can be changed by varying the macroscopic stresses Σ_{ij}^α and Σ_c^α. For increments of Σ_{ij} and Σ_c the virtual work expression becomes:

$$d\Sigma_{ij}^\alpha \dot{E}_{ij}^\alpha - d\Sigma_c^\alpha \dot{f}_V^\alpha = \frac{1}{V} \int_V d\sigma_{ij} \dot{\varepsilon}_{ij} \, dV = \frac{1}{V} \int_V d\sigma_{ij} \frac{\partial \phi}{\partial \sigma_{ij}} \, dV$$

$$= \frac{1}{V} \int_V d\phi \, dV = d\Phi^\alpha \tag{3.5}$$

Therefore

$$\dot{E}_{ij}^\alpha = \frac{\partial \Phi^\alpha}{\partial \Sigma_{ij}^\alpha} \tag{3.6a}$$

and
$$\dot{f}_V^\alpha = - \frac{\partial \Phi^\alpha}{\partial \Sigma_c^\alpha} \tag{3.6b}$$

where Φ is a scalar function of Σ_{ij}^{α}, Σ_{c}^{α} and f_{V}^{α}.

The result of equation (3.6a) is due to Duva and Hutchinson [13]. Inclusion of the surface tension term leads to the additional result of eqn. (3.6b). Surface tension does not strongly influence the form of the potential but its inclusion leads to a compact form of the constitutive equation. The effect of surface energy can be easily included in the work of Duva and Hutchinson [13] who obtain expressions for Φ for dilute volume fractions of voids. Another method of finding Φ is to use extremum theorems [14,15] to obtain bounds on Φ. This approach allows the analysis of concentrated as well as dilutely voided materials [16].

Although it has proved convenient to develop the constitutive model in terms of the volume fraction of voids in the grain-boundary elements, when comparing the different mechanisms of void growth it is more advantageous to express the equations in terms of the area fraction of voids in the plane of the grain-boundary, f_{h}^{α} :

$$f_{h}^{\alpha} = \left(\frac{r_{h}^{\alpha}}{\ell^{\alpha}}\right)^{2} = \left(\frac{3}{2}\right)^{2/3} f_{V}^{\alpha\,2/3} \tag{3.7a}$$

We can define an associated internal stress

$$\Sigma_{h}^{\alpha} = \frac{2\gamma_{s}}{\ell^{\alpha}} = \left(\frac{3}{2}\right)^{2/3} \Sigma_{c}^{\alpha}\, f_{V}^{\alpha\,1/3} \tag{3.7b}$$

Now combining eqns. (3.6b) and (3.7) we find

$$\dot{f}_{h}^{\alpha} = \left(\frac{2}{3}\right)^{1/3} f_{V}^{\alpha\,-1/3}\, \dot{f}_{V}^{\alpha} = -\left(\frac{2}{3}\right)^{1/3} f_{V}^{\alpha\,-1/3}\, \frac{\partial \Phi_{c}^{\alpha}}{\partial \Sigma_{c}^{\alpha}}$$

$$= -\frac{\partial \Phi_{c}^{\alpha}}{\partial \Sigma_{c}^{\alpha}} \frac{\partial \Sigma_{c}^{\alpha}}{\partial \Sigma_{h}^{\alpha}}$$

$$= - \frac{\partial \bar{\Phi}_c^{\alpha}}{\partial \Sigma_h^{\alpha}} \qquad (3.8)$$

The important point about the above result is that the internal damage variable is non unique. We could choose any function of the volume fraction, f_V^{α}, to describe the damage and still obtain the general form of result of eqn. (2.15).

3.2 Void Growth by Grain-Boundary Diffusion

At low stresses, deformation due to power-law creep is slow and the mechanism of void growth changes to one directly controlled by the diffusion of material. A void grows by material diffusing along its surface by surface diffusion to the grain-boundary. It then flows along the grain boundary where it is uniformly deposited, Fig. 5. These are two sequential processes, so it is the slower one that determines the overall rate of growth. In this subsection we consider the situation where the void growth is limited by the rate of grain-boundary diffusion, and in the next subsection we examine the conditions when surface diffusion controls the rate of growth.

For simplicity we assume that the grain-boundary energy is the same as that of a perfect crystal, so that the voids remain spherical as they grow. Again we isolate a grain-boundary element of material, Fig. 2, and perform the analyses in terms of the local stress field. The conceptual reversible path we follow in defining the free energy requires making a cut along the grain boundary, Fig. 6. Material is then scooped out to form the voids, which is spread evenly along the grain boundary. The surfaces are then rejoined and the resulting change in free energy is

$$\phi = 3 f_v^{\alpha 2/3} \gamma_s A_{\alpha}$$

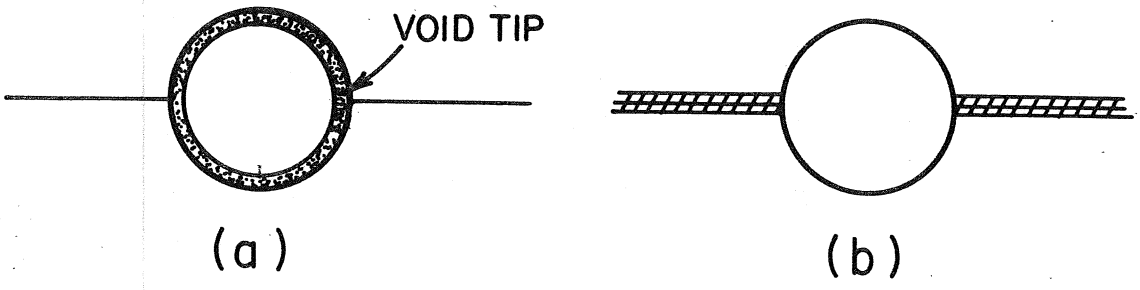

Fig. 5. The void grows by material flowing along its surface to the tip and then along the grain boundary where it is uniformly plated. In this process the shaded region in (a) is transported to the shaded area of (b).

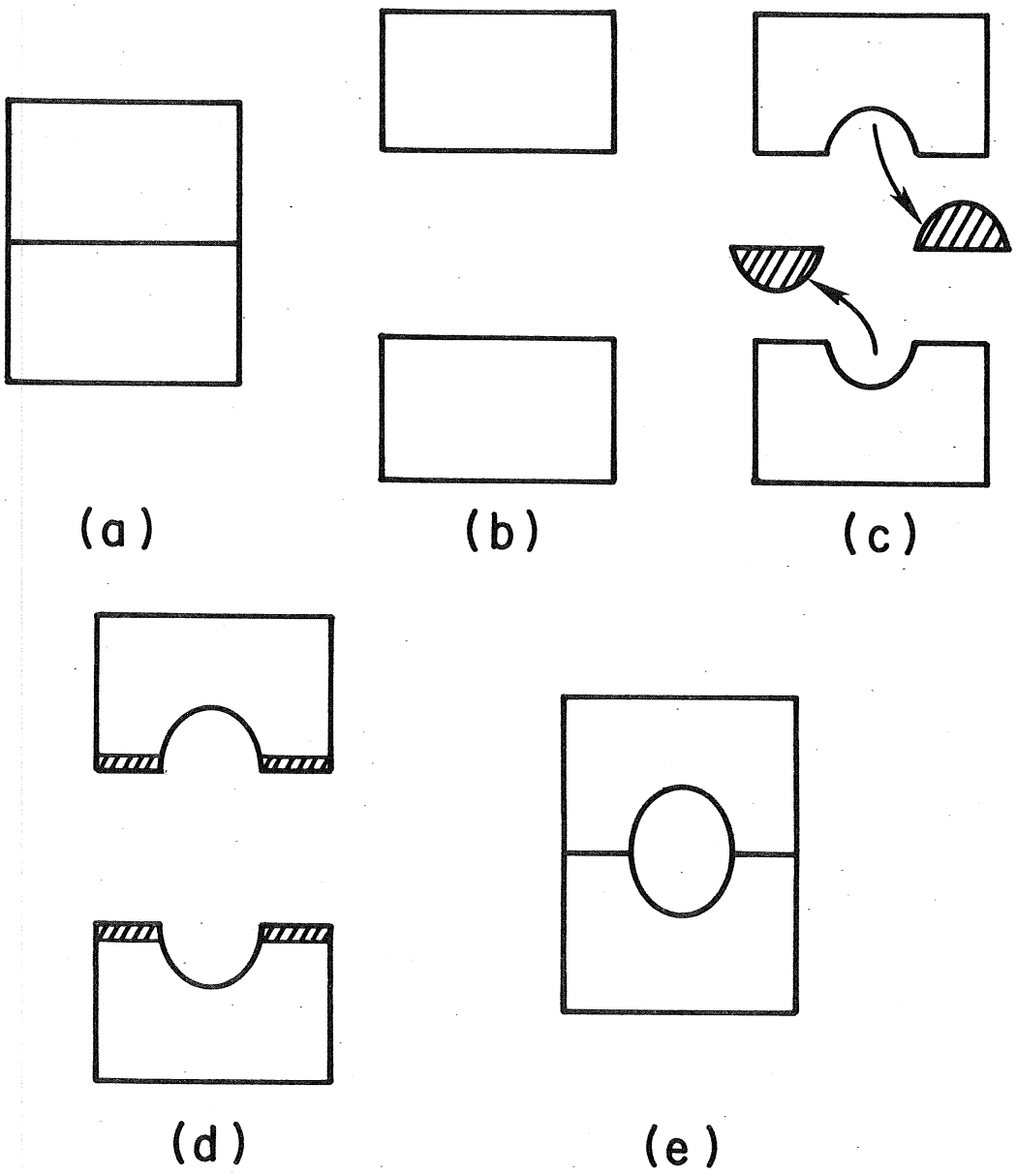

Fig. 6. Conceptual reversible process of forming a void on the grain boundary: (a) initial void free material; (b) a cut is made along the grain boundary; (c) material is scooped out to form a void; (d) this material is spread evenly along the grain boundary; (e) the two pieces of material are rejoined.

where A_α is the grain-boundary area.

Application of the stress Σ_{ij}^α gives the total free energy

$$\psi = \frac{1}{2} C_{ijk\ell}^\alpha E_{k\ell}^{e\alpha} E_{ij}^{e\alpha} V_\alpha + 3 f_v^{\alpha 2/3} \gamma_s A_\alpha \qquad (3.9)$$

Duva and Hutchinson [13] give $C_{ijk\ell}^\alpha$ for a dilute volume fraction of voids in an incompressible elastic material. Cocks [16] gives an approximate result for any volume fraction:

$$C_{ijk\ell}^\alpha = \frac{2}{3} E(1 - f_v^\alpha) \delta_{ik} \delta_{j\ell} + \frac{4}{9} \frac{E(1-f_v^\alpha)}{f_v^\alpha} \delta_{ij} \delta_{k\ell} \qquad (3.10)$$

where δ_{ij} is the Kronecker delta and E is Young's modulus.

Differentiating eqn. (3.9) gives the Affinities

$$\frac{\partial \psi}{\partial E_{ij}^e} = \Sigma_{ij}^\alpha V_\alpha \qquad (3.11)$$

$$\frac{\partial \psi}{\partial f_v^\alpha} = - \left[\frac{1}{2} \frac{\Sigma_e^{\alpha 2}}{E(1 - f_v^\alpha)^2} + \frac{9}{8} \frac{\Sigma_m^{\alpha 2}}{E(1 - f_v^\alpha)^2}\right] V_\alpha + \frac{2\gamma_s A_\alpha}{f_v^{1/3}} \qquad (3.12)$$

where Σ_e^α is the von Mises effective stress $\Sigma_e^{\alpha 2} = \frac{3}{2} S_{ij}^\alpha S_{ij}^\alpha$, Σ_m^α is the mean stress $\Sigma_m^\alpha = \frac{1}{3} \Sigma_{kk}^\alpha$, and S_{ij}^α is the deviatoric component of stress $S_{ij}^\alpha = \Sigma_{ij}^\alpha - \Sigma_m^\alpha \delta_{ij}$.

The second law of thermodynamics, eqn. (2.6) then becomes

$$\Sigma_{ij}^{\alpha p} \dot{E}_{ij}^{\alpha p} - \left(\Sigma_c^\alpha - \left(\frac{1}{2} \frac{\Sigma_e^{\alpha 2}}{E(1 - f_v^\alpha)} + \frac{9}{8} \frac{\Sigma_m^{\alpha 2}}{E(1 - f_v^\alpha)^2}\right)\right) \dot{f}_v^\alpha \geq 0 \qquad (3.13)$$

where

$$\Sigma_c^\alpha = \frac{2\gamma_s}{r_h}$$

The inelastic strain-rate, $\dot{E}^{\alpha p}_{ij}$, results from the plating of material onto the grain boundary. The rate of thickening of the grain boundary, $\dot{v}_i$, is directly proportional to the rate of increase of the volume of the voids:

$$\dot{v}_i = 2\dot{f}^{\alpha}_{v}\, \ell^{\alpha}\, n^{\alpha}_{i} \tag{3.14}$$

The inelastic strain-rate can then be obtained from the kinematic relationship (see Appendix)

$$\dot{E}^{\alpha p}_{ij} = \frac{1}{4\ell^{\alpha}} (\dot{v}_i\, n^{\alpha}_{j} + \dot{v}_j\, n^{\alpha}_{i}) \tag{3.15}$$

Combining eqns. (3.14) and (3.15) gives $\dot{E}^{\alpha p}_{ij}$ in terms of $\dot{f}^{\alpha}_{v}$:

$$\dot{E}^{\alpha p}_{ij} = \dot{f}^{\alpha}_{v}\, n^{\alpha}_{i}\, n^{\alpha}_{j} \tag{3.16}$$

This expression is equivalent to eqn. (2.8) of section 2, where

$$g_k \equiv n^{\alpha}_{i}\, n^{\alpha}_{j}$$

Equation (3.16) can be substituted into eqn. (3.13) to give the rate of energy dissipation,

$$\{(\Sigma^{\alpha}_{ij}\, n^{\alpha}_{i}\, n^{\alpha}_{j} - \Sigma^{\alpha}_{c}) + [\frac{1}{2} \frac{{\Sigma^{\alpha}_{e}}^2}{E(1 - f^{\alpha}_{v})^2} + \frac{9}{8} \frac{{\Sigma^{\alpha}_{m}}^2}{E(1 - f^{\alpha}_{v})^2}]\}\ \dot{f}^{\alpha}_{v} \geq 0 \tag{3.17}$$

This mechanism tends to dominate at stress levels where $\frac{\Sigma}{E} < 10^{-3}$, so that the term in the square brackets, which scales as $\frac{\Sigma^2}{E}$, is always much smaller than the other terms, which scale as Σ , and can be ignored. Eqn. (3.17) then becomes

$$(\Sigma^{\alpha}_{ij}\, n^{\alpha}_{i}\, n^{\alpha}_{j} - \Sigma^{\alpha}_{c})\ \dot{f}^{\alpha}_{v} \geq 0 \tag{3.18}$$

The component of stress $\Sigma^{\alpha}_{ij}\, n^{\alpha}_{i}\, n^{\alpha}_{j}$ is simply the stress normal to the grain boundary.

A detailed analysis of this mechanism of void growth gives a growth rate [12,17]

$$\dot{f}^{\alpha}_{v} = \frac{\Omega(\Sigma^{\alpha}_{ij}\, n^{\alpha}_{i}\, n^{\alpha}_{j} - \Sigma^{\alpha}_{c})}{2\ell^{\alpha^3}\, f^{\alpha}_{v}\, \ell n\, 1/f^{\alpha}_{v}} \tag{3.19}$$

where Ω is a temperature dependent material parameter. This expression is of the form, eqn. (2.10), which allows us to prove the existence of a scalar potential, Φ^{α}_{v}, such that

$$\dot{E}^{\alpha p}_{ij} = \frac{\partial \Phi^{\alpha}_{v}}{\partial \Sigma^{\alpha}_{ij}}$$

and

$$\dot{f}^{\alpha}_{v} = -\frac{\partial \Phi^{\alpha}_{v}}{\partial \Sigma^{\alpha}_{c}} \tag{3.20}$$

Following the analysis leading to eqn. (3.8) we can express the potential in terms of the area fraction of voids f^{α}_{h} instead of f^{α}_{v} and define a stress $\Sigma^{\alpha}_{h} = \frac{2\gamma_s}{\ell^{\alpha}}$, such that

$$\dot{f}^{\alpha}_{h} = -\frac{\partial \Phi^{\alpha}_{v}}{\partial \Sigma^{\alpha}_{h}} \tag{3.21}$$

3.3 Void Growth Limited by Surface Diffusion

In the last subsection we assumed that surface diffusion was sufficiently fast for the void to maintain a spherical shape as it grew. When the rate of surface diffusion is slower than grain-boundary diffusion material cannot be supplied fast enough to the tip of the growing void. Material is then only removed from the void tip region, and the void adopts a crack like profile as

it grows. The detailed shape of the growing void is now a function of the history of loading, but the rate of void growth is only a function of the shape of the crack-tip region [12,18].

Here we limit our attention to the steady state process of void growth at constant stress and assume that the new steady state is soon reached when the stress is changed. We can now define the state of the material surrounding a given grain-boundary using two internal state variables: the volume fraction of voids in the grain boundary element, f_v^α, through which we relate the inelastic strain; the area fraction of voids, f_h^α, in the plane of the grain boundary, which we use as a measure of the surface area of the voids. What we have described so far is the material response to a tensile stress normal to the plane of the grain boundary. When this stress is compressive the void profile is completely different, Fig. 7, and if the stress is changed from tension to compression the transient response before reaching the new steady state can be significant. In the present section we limit our attention to tensile stresses, although similar expressions can be derived for compression.

At a given instant the free energy can be obtained by again following the reversible process of Fig. 6:

$$\psi = \frac{1}{2} C^\alpha_{ijk\ell} E^{\alpha e}_{k\ell} E^{\alpha e}_{ij} V_\alpha + 2f^\alpha_h \gamma_s A_\alpha \qquad (3.22)$$

This expression is similar to eqn. (3.9) of the last subsection. The second term on the r.h.s. arises from the introduction of free surfaces in the material when the voids are formed. In practice the contribution from this effect is also a function of f_v^α and the history of loading, but in most practical situations the dependence on these variables is weak, and the simple form of eqn. (3.22) is sufficient.

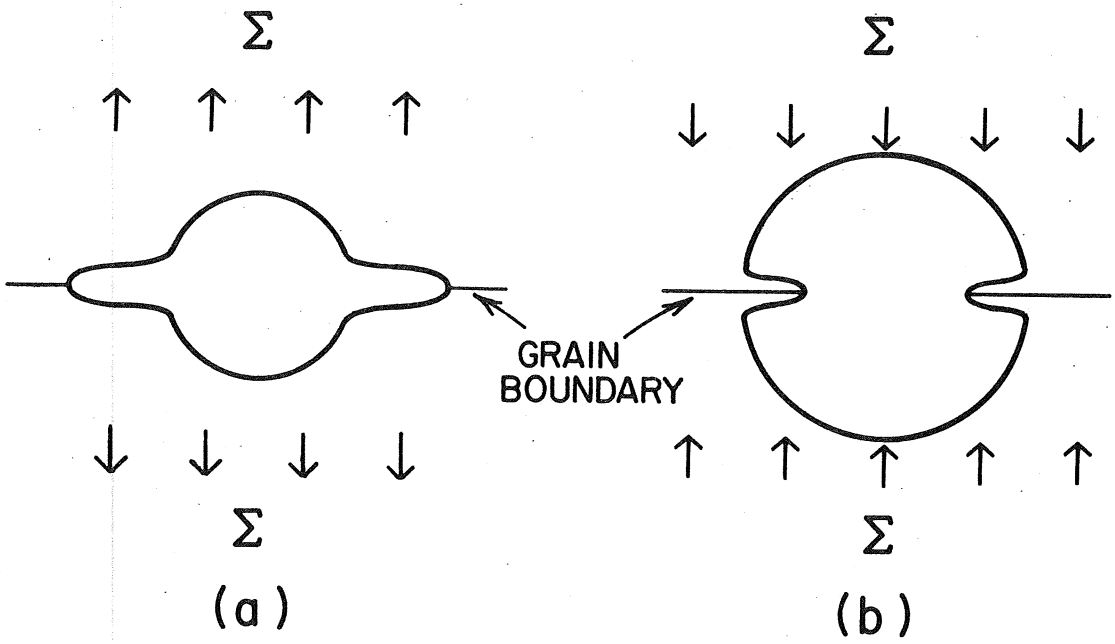

Fig. 7. (a) Shape adopted by growing void for tensile stress across the grain-boundary in the limit of surface diffusion controlled growth. (b) Shape adopted by sintering void for compressive loading.

Differentiation of eqn. (3.22) gives the thermodynamic forces

$$\frac{\partial \psi}{\partial E_{ij}^{\alpha e}} = \Sigma_{ij}^{\alpha} V_{\alpha} \tag{3.23}$$

$$\frac{\partial \psi}{\partial f_h^{\alpha}} = 2\gamma_s A_{\alpha} \tag{3.24}$$

In the derivation of the above equation the variation of $C_{ijk\ell}^{\alpha}$ with both f_v^{α} and f_h^{α} has been neglected, since, as in the last section, the effect is small.

The second law, eqn. (2.6), now becomes

$$\Sigma_{ij}^{\alpha p} \dot{E}_{ij}^{\alpha p} V_{\alpha} - 2\gamma_s A_{\alpha} \dot{f}_h^{\alpha} \geq 0 \tag{3.25}$$

As before the inelastic strain-rate, $\dot{E}_{ij}^{\alpha p}$, is related to $\dot{f}_v^{\alpha}$ through eqn. (3.16) and eqn. (3.24) becomes

$$\Sigma_{ij}^{\alpha} n_i^{\alpha} n_j^{\alpha} \dot{f}_v^{\alpha} V_{\alpha} - 2\gamma_s A_{\alpha} \dot{f}_h^{\alpha} \geq 0$$

or

$$\Sigma_{ij}^{\alpha} n_i^{\alpha} n_j^{\alpha} \dot{f}_v^{\alpha} - 3\Sigma_h^{\alpha} \dot{f}_h^{\alpha} \geq 0 \tag{3.26}$$

where

$$\Sigma_h^{\alpha} = \frac{2\gamma_s}{3\ell^{\alpha}}$$

Chuang et al. [18] have analyzed this mechanism in detail. They show that for steady state growth

$$\dot{f}_v^{\alpha} = \frac{f_h^{\alpha\ 1/2}}{(1 - f_h^{\alpha})^3} 3\Sigma_h^{\alpha} \Delta (\Sigma_{ij}^{\alpha} n_i^{\alpha} n_j^{\alpha})^2 \tag{3.27}$$

$$\dot{f}_h^{\alpha} = \frac{f_h^{\alpha\ 1/2}}{(1 - f_h^{\alpha})^3} \Delta (\Sigma_{ij}^{\alpha} n_i^{\alpha} n_j^{\alpha})^3 \tag{3.28}$$

where Δ is a temperature dependent material property. If we substitute these expressions into eqn. (3.26) we find that

$$\Sigma_{ij}^{\alpha}\ n_i^{\alpha}\ n_j^{\alpha}\ \dot{f}_v^{\alpha} = 3\Sigma_h^{\alpha}\ \dot{f}_h^{\alpha} \tag{3.29}$$

i.e. the work done by the applied load all goes into creating the new crack surfaces.

Eqn. (3.27) is in the form of eqn. (2.10):

$$\dot{f}_v^{\alpha} = \dot{f}_v^{\alpha}\ (F_v^{\alpha},\ \Sigma_h^{\alpha},\ f_h^{\alpha}) \tag{3.30}$$

where

$$F_v^{\alpha} = \Sigma_{ij}^{\alpha}\ n_i^{\alpha}\ n_j^{\alpha}$$

Following the analysis of section 2 we can prove the existence of a scalar potential Φ^v such that

$$\dot{E}_{ij}^{\alpha p} = \frac{\partial \Phi_v^{\alpha}}{\partial \Sigma_{ij}^{\alpha}} \tag{3.31}$$

and

$$\dot{f}_v^{\alpha} = -\frac{\partial \Phi_v^{\alpha}}{\partial F_v^{\alpha}} \tag{3.32}$$

When considering the life of a component f_h^{α} is a more important variable than f_v^{α}, because failure occurs when the voids have linked to form a crack. This occurs when $f_h^{\alpha} = 1$, and the value of f_v^{α} at this instant is unimportant. Eqn. (3.29) gives a relationship between $\dot{f}_v^{\alpha}$ and $\dot{f}_h^{\alpha}$. Combining this with eqn. (3.32) gives

$$\dot{f}_h^{\alpha} = \dot{f}_v^{\alpha}\ \frac{F_v^{\alpha}}{3\Sigma_h^{\alpha}} \equiv -\frac{\partial \Phi_v^{\alpha}}{\partial \Sigma_h^{\alpha}} \tag{3.33}$$

So that the strain-rate and rate of increase of $\dot{f}_h^{\alpha}$ are again derivable from

the same potential.

3.4 Grain-boundary Sliding

In the previous three sub-sections it was shown that when voids grow within an element of material it is possible to prove the existence of a scalar potential from which the inelastic strain-rate and rate of growth of the voids can be derived. Also the strain-rate of a void free element of material is given by the potential form of eqn. 3.1. Another contribution to the inelastic strain-rate arises from grain-boundary sliding in the material. Here we analyse this contribution to the deformation of the material. Any arbitrary amount of sliding in the grain boundary can be divided into components u_s^α in the $\underline{s}^\alpha$ direction and u_t^α in the direction of $\underline{t}^\alpha$, Fig. 2. There is no change of internal structure when sliding occurs, so u_s^α and u_t^α are not state variables, but their rate of change gives the speed of the process. If we assume that the size of the voids remains constant then the only contribution to the free energy is the elastic stored energy which results from deforming the material elastically:

$$\psi = \frac{1}{2} C^\alpha_{ijk\ell} E^{e\alpha}_{ij} E^{e\alpha}_{ij} V_\alpha$$

Differentiating the above equation and substituting the result into eqn. (2.6) gives the rate of energy dissipation

$$\Sigma^\alpha_{ij} \dot{E}^{s\alpha}_{ij} \geq 0$$

$\dot{E}^{s\alpha}_{ij}$ is the inelastic strain-rate which is related to the rate of change of internal variables through the kinematic relationship

$$\dot{E}^{\alpha s}_{ij} = \frac{1}{4\ell^{\alpha}} [\dot{u}^{\alpha}_{i} n^{\alpha}_{j} + \dot{u}^{\alpha}_{j} n^{\alpha}_{i}]$$

$$= \frac{1}{4\ell^{\alpha}} [\dot{u}^{\alpha}_{s} (s^{\alpha}_{i} n^{\alpha}_{j} + s^{\alpha}_{j} n^{\alpha}_{i}) + \dot{u}^{\alpha}_{t} (t^{\alpha}_{i} n^{\alpha}_{j} + t^{\alpha}_{j} n^{\alpha}_{i})]$$

This equation is equivalent to eqn. (2.8) of section 2, although now the internal displacement rates are not state variables changing, they are a measure of the rate of the irreversible process:

$$\frac{\tau_{sn}}{2\ell^{\alpha}} \dot{u}^{\alpha}_{s} + \frac{\tau_{tn}}{2\ell^{\alpha}} \dot{u}^{\alpha}_{t} \geq 0$$

where
$$\tau_{sn} = \frac{1}{2} \Sigma^{\alpha}_{ij} (s^{\alpha}_{i} n^{\alpha}_{j} + s^{\alpha}_{j} n^{\alpha}_{i})$$

and
$$\tau_{tn} = \frac{1}{2} \Sigma^{\alpha}_{ij} (t^{\alpha}_{i} n^{\alpha}_{j} + t^{\alpha}_{j} n^{\alpha}_{i}) \qquad (3.34)$$

are the shear components of the remote stress Σ^{α}_{ij} in the directions of u^{α}_{s} and u^{α}_{t} respectively. It is conventional to assume that the sliding rates $\dot{u}^{\alpha}_{t}$ and $\dot{u}^{\alpha}_{t}$ are linear functions of their resolved shear stresses. These relationships are of the general form of eqn. (2.10), so that it is possible to prove the existence of a potential, Φ^{α}_{s} (eqn. 2.15), such that

$$\dot{E}^{\alpha s}_{ij} = \frac{\partial \Phi^{\alpha}_{s}}{\partial \Sigma^{\alpha}_{ij}} \qquad (3.35)$$

where $\Phi^{\alpha}_{s} = \frac{\tau^{2}_{max}}{4\ell^{\alpha}\eta}$ and η is a material constant. $\tau_{max} = (\tau^{2}_{sn} + \tau^{2}_{tn})^{1/2}$ is the maximum resolved shear stress in the plane of the grain boundary.

When grain boundaries slide freely they are unable to support any shear stresses and complex stress states can develop in a material even under simple loading conditions. In section 7 we see that an effect of this is to magnify

the stress transmitted across certain grain boundaries.

3.5 Deformation rate of macroscopic element of material

The general situation considered in this section is shown in Fig. 1. In each grain-boundary element there are two contributions to the inelastic strain-rate: from void growth and grain-boundary sliding. The contribution from void-growth is given by one of eqns. (3.6), (3.20) or (3.31) and that from grain-boundary sliding by eqn. (3.35). Making use of eqn. (2.21) these eqns. can be combined with eqn. (3.1) to give the macroscopic potential $\overline{\Phi}$:

$$\dot{E}^p_{ij}\, d\Sigma_{ij} - \sum_\alpha \dot{f}^\alpha_h\, d\Sigma^\alpha_h\, v_\alpha = \frac{1}{V}\int_{V_g} d\phi\, dV + \sum_\alpha d\Phi^\alpha_c\, v_\alpha + \sum_\alpha d\Phi^\alpha_s\, v_\alpha = d\overline{\Phi} \quad (3.36)$$

where V_g is the volume of material outside of the grain-boundary regions.

Then
$$\dot{E}^p_{ij} = \frac{\partial\overline{\Phi}}{\partial\Sigma_{ij}} \quad (3.37)$$

and each $\dot{f}^\alpha_h$ is given by

$$\dot{f}^\alpha_h = -\frac{1}{v_\alpha}\frac{\partial\overline{\Phi}}{\partial\Sigma^\alpha_h} \quad (3.38)$$

4. Nucleation of Cavities

In the last section we assumed that the number and spacing of cavities remained fixed throughout the life of a component. In practice cavities nucleate continuously during the lifetime resulting in a gradual decrease of their spacing and an enhancement of the growth rate of the other cavities, eqn. (3.19). The processes by which cavities nucleate are not fully understood at the present time, but most recent studies of the subject follow the analysis of Raj and Ashby [19] in assuming that cavities form due to the coalescence of vacancies in the material. Such analyses lead to a threshold

stress for nucleation. Below this stress the rate of nucleation is so slow that it can be assumed that voids never nucleate, while above this stress the rate of nucleations is so fast that it can be assumed that voids nucleate as soon as the threshold stress is exceeded. All studies to date predict values of the threshold stress which are much greater than the applied stresses used in the majority of creep experiments [20]. Attention has therefore focused on ways in which these high levels of stress concentration can be achieved in the material [20,21,22]. Argon et al [20] and Wang et al [21] show how the level of stress concentration can be achieved during grain-boundary sliding, while Cocks [22] demonstrates how differences between the diffusion characteristics of the grain-boundary and particle-matrix interface can lead to high stress concentration. Neither approach leads to satisfactory explanations of the nucleation process. It is evident that further experimental and theoretical studies are requird to clarify the problem.

In this section we outline the approach of Raj and Ashby [19] and show that a potential exists from which the inelastic strain-rate can be derived. Also, in the simplified situation considered here, the rate of nucleation and void-growth rate are derivable from the same potential.

Consider the situation for which a grain-boundary element of material contains a number n_s of potential sites for the nucleation of voids. At a given instant in time the material contains an area fraction f_h^α of voids which are growing on n of the nucleation sites. Within an element of material we now have two state variables, f_h^α and n.

When calculating the contribution to the free energy from the nucleation of the cavities the reversible process outlined in Fig. 6 can again be followed. Material can be scooped from the nucleation site and spread onto the grain-boundary. In the process the stress normal to the grain-boundary

does work and the internal surface, and hence the total surface energy, increases. Consequently part of the volume of the void at a given instant can be assigned to the nucleation process and the remainder to the growth process.

In the early stages of void growth the rate of growth is generally controlled by grain-boundary diffusion. Examination of eqn. (3.19) then reveals that a void must have a radius

$$r_c^\alpha = \frac{2\gamma_s}{\Sigma_{ij}^\alpha n_i^\alpha n_j^\alpha} \tag{4.1}$$

before it can grow. Problems arise in choosing a small number of state variables when we allow the voids to nucleate continuously. We will assume however that we can, at least approximately, characterize the material response in terms of f_h^α and n, so that the free energy expression takes the form

$$\phi^\alpha = \phi^\alpha(E_{ij}^{e\alpha},\ f_h^\alpha,\ n) \tag{4.2}$$

and

$$\dot{\phi}^\alpha = \frac{\partial\phi^\alpha}{\partial E_{ij}^{e\alpha}} \dot{E}_{ij}^{e\alpha} + \frac{\partial\phi^\alpha}{\partial f_h^\alpha} \dot{f}_h^\alpha + \frac{\partial\phi^\alpha}{\partial n^\alpha} \dot{n}^\alpha$$

$$= \Sigma_{ij} \dot{E}_{ij}^{e\alpha} + \Sigma_h^\alpha \dot{f}_h^\alpha + \Sigma_n^\alpha \dot{n}_\alpha \tag{4.3}$$

where

$$\Sigma_n^\alpha = \frac{\partial\phi^\alpha}{\partial n^\alpha}$$

Equation (2.6) then becomes

$$\Sigma_{ij}^\alpha \dot{E}_{ij}^{p\alpha} - S_h^\alpha \dot{f}_h^\alpha - S_n^\alpha \dot{n}^\alpha \geqslant 0 \tag{4.4}$$

Now part of the inelastic strain rate, $\dot{E}_{ij}^{p\alpha}$ results from the nucleation of the voids, $\dot{E}_{ij}^{n\alpha}$, and the remainder, $\dot{E}_{ij}^{h\alpha}$, from their growth. Equation (4.4)

then becomes

$$(\Sigma_{ij}^{\alpha}\ \dot{E}_{ij}^{h\alpha} - S_h^{\alpha}\ \dot{f}_h^{\alpha}) + (\Sigma_{ij}^{\alpha}\ \dot{E}_{ij}^{n\alpha} - S_n^{\alpha}\ \dot{n}^{\alpha}) \geq 0 \qquad (4.5)$$

and since the nucleation and growth processes can occur independently of each other, each of the bracketed terms above must be greater than or equal to zero. We examined the first of these terms in the previous section and showed that a potential exists from which the inelastic strain-rate and rate of increase of area fraction of voids can be derived, eqn. (3.20). This potential contains the number of voids $[n^{\alpha} = 1/\ell^{\alpha}2]$ which is now a variable, i.e. the potential

$$\phi_v^{\alpha} = \phi_v^{\alpha}\ (\Sigma_{ij}^{\alpha},\ \Sigma_h^{\alpha},\ f_h^{\alpha},\ n^{\alpha}) \qquad (4.6)$$

The approach used in analysing thermally activated processes such as the nucleation of voids differs slightly from that described in section 2. The change in entropy associated with the random nucleation of voids becomes important in determining the response of the material. It is conventional to omit the entropy term from the expression for the free energy and include its effect as a kinetic relationship for the rate of nucleation, which is largely phenomenological. The effect of this is that the rate of energy dissipation given by eqn. (4.5) is less than zero. This energy must be supplied through thermal fluctuations, which is incorporated in the entropy terms. The term

$$\Sigma_{ij}^{\alpha}\ \dot{E}_{ij}^{n\alpha} - S_n^{\alpha}\ \dot{n}^{\alpha}$$

of eqn. (4.5) can be expressed as

$$(\Sigma_{ij}^{\alpha}\ B_{ij}^{\alpha} - S_n^{\alpha})\ \dot{n}^{\alpha}$$

since $\dot{E}^{n\alpha}_{ij} = B^{\alpha}_{ij}\ \dot{n}^{\alpha}$ results directly from the nucleation of the voids. As before the term $(\Sigma^{\alpha}_{ij}\ B^{\alpha}_{ij} - S^{\alpha}_{n})$ (which is now negative) can be interpreted as a driving force for nucleation, it is a measure of the additional energy required from thermal fluctuations which is incorporated in the entropy expressions. If this is a small negative quantity then the rate of nucleation is fast but if it is large the rate of nucleation is slow.

It is instructive to consider the nucleation process in slightly more detail. We are interested in the situation when a grain-boundary contains n_s possible nucleation sites per unit area. When a void of critical radius r^{α}_{c} forms at one of these sites there is an increase in the free energy due to the formation of the new surface. The free energy is then (excluding the contribution from the entropy)

$$\phi = \frac{1}{2}\ C_{ijk\ell}\ E^{e\alpha}_{k\ell}\ E^{e\alpha}_{ij}\ V + 4\pi r_c^2\ \gamma_s\ n \tag{4.7}$$

where it has been assumed that the voids that form are spherical. Differentiation of eqn. (4.7) then gives

$$\dot{\phi} = \Sigma^{\alpha}_{ij}\ \dot{E}^{e\alpha}_{ij}\ V + 4\pi r_c^2\ \gamma_s\ \dot{n} \tag{4.8}$$

where the change in stiffness due to the formation of the voids has been ignored since it is always small compared to the other terms and r_c has been taken as a constant. The rate of energy dissipation, eqn. (2.7), then becomes

$$\dot{D} = \Sigma^{\alpha}_{ij}\ \dot{E}^{p\alpha}_{ij}\ V - 4\pi r_c^2\ \gamma_s\ \dot{n} \tag{4.9}$$

where the inelastic strain-rate

$$\dot{E}^{p\alpha}_{ij} = \frac{\dot{n}^{\alpha}}{V^{\alpha}}\ \frac{4}{3}\ \pi\ r_c^3\ n^{\alpha}_{i}\ n^{\alpha}_{j} \tag{4.10}$$

Substituting this into eqn. (4.9) gives

$$\dot{D} = (\Sigma^{\alpha}_{ij}\ n_i n_j\ \frac{4}{3}\ \pi r_c^3 - 4\pi r_c^2\ \gamma_s)\ \dot{n}^{\alpha}$$

$$= F^{\alpha}_{n}\ \dot{n}^{\alpha} \qquad (4.11)$$

Analyses of the nucleation process [19,22] give

$$\dot{n}^{\alpha} = (n^{\alpha}_{s} - n^{\alpha})\ A \exp \frac{F^{\alpha}_{n}}{RT} \qquad (4.12)$$

where A is a temperature dependent material property and n^{α}_{s} is the number of potential nucleation sites. This equation is of the form of eqn. (2.10), and eqn. (4.10) is equivalent to eqn. (2.8), so that it is possible to prove the existence of a scalar potential, Φ^{α}_{n}, from which the strain-rate and rate of nucleation can be derived:

$$\dot{E}^{p\alpha}_{ij} = \frac{\partial \Phi^{\alpha}_{n}}{\partial \Sigma^{\alpha}_{ij}}$$

$$\dot{n}^{\alpha} = \frac{\partial \Phi}{\partial F_{\alpha}} = -\frac{\partial \phi}{\partial S^{\alpha}_{n}}$$

where

$$S^{\alpha}_{n} = 4\pi r_c^2\ \gamma_s$$

The total strain-rate and damage rates $\dot{f}^{\alpha}_{h}$ and $\dot{n}^{\alpha}$ are derivable from the potential

$$\Phi^{\alpha} = \Phi^{\alpha}_{v} + \Phi^{\alpha}_{n}$$

It was stated earlier that this approach to void nucleation leads essentially to a threshold stress for nucleation. We can apply the above analysis to small regions of grain boundaries, where the local stress depends on the interaction of these individual elements. The stresses change continually and once the threshold stress is reached locally voids can nucleate and grow, the stress is then shed onto other regions where further

nucleation can occur. In this way it is possible to obtain a continuous nucleation of voids as the material creeps. As in the last section the damage potentials Φ_n^α can be combined with the sliding potentials Φ_s^α and the potentials for the grain interiors to give a global macroscopic potential from which the strain-rate and damage rate can be derived.

5. The Use of Average Quantities

In the previous sections we developed the thermodynamic description of the material in terms of discrete state variables. Rice [1] describes how the thermodynamics can be expressed in terms of average quantities. Here, instead, we make use of a result due to Onat and Leckie [7] in expressing the distribution of cavitated boundaries in terms of a series of even order tensors. The potential can then be expressed in terms of these tensors, whose rates are derivable from it.

Following Onat and Leckie [7] we now define a grain-boundary in terms of the outward normals on either side of the boundary. We further assume that there is no anisotropy in the distribution of grain-boundaries, and that all boundaries with the same outward normal contain the same area fraction of voids, f_h^α (here we use f_h^α instead of f_v^α, so that we can combine the various mechanisms of void growth) and for simplicity we assume that the voids are all present at the beginning of the life. If one end of an outward normal is placed at the origin of a linear co-ordinate system, the other end lies at a point on a sphere, s, of unit radius, Fig. 8. We can extend this line beyond s by an amount which scales as the area fraction of voids on the grain boundaries represented by the outward normal. The surface, Γ, formed by the tips of these lines is symmetric about any diameter since a mirror image is formed when the second normal is drawn in the opposite direction.

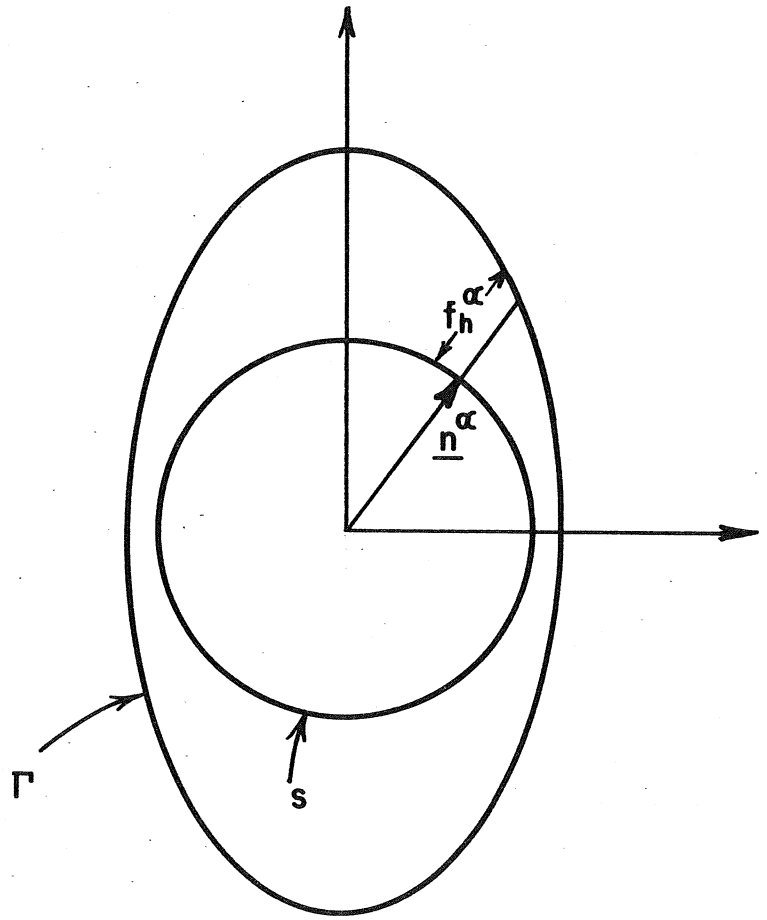

Fig. 8. The surface Γ is the locus of the end points of a series of radial lines of length f_h^α in the direction of $\underline{n}^\alpha$, which orginate on a sphere of unit radius, s.

Onat and Leckie [7] show that the shape of Γ can be described by a series of even order tensors:

$$D = \frac{1}{4\pi} \int_S f_h^\alpha \, ds$$

$$D_{ij} = \frac{15}{8\pi} \int_S f_v^\alpha \, (n_i n_j - \frac{1}{3} \delta_{ij}) ds \tag{5.1}$$

$$D_{ijk\ell} = \frac{315}{32\pi} \int_S f_v^\alpha \, \kappa_{ijk\ell} \, ds$$

etc.

where $$\kappa_{ijk\ell} = n_i n_j n_k n_\ell - \frac{1}{7} (\delta_{ij} \, n_k n_\ell + \delta_{ik} \, n_j n_\ell + \delta_{i\ell} \, n_j n_k$$

$$+ \delta_{jk} \, n_i n_\ell + \delta_{j\ell} \, n_i n_k + \delta_{k\ell} \, n_i n_k + \delta_{k\ell} \, n_i n_j)$$

$$+ \frac{1}{35} (\delta_{ij} \, \delta_{k\ell} + \delta_{ik} \, \delta_{j\ell} + \delta_{i\ell} \, \delta_{jk}) \, . \tag{5.2}$$

All odd order tensors are zero because of the symmetry of Γ.

Onat and Leckie [7] further show that the damage on each grain boundary can be written in terms of these tensors

$$f_h^\alpha = D + D_{ij} \, (n_i n_j - \frac{1}{3} \delta_{ij}) + D_{ijk\ell} \, \kappa_{ijk\ell} + \cdots \tag{5.3}$$

In the last three sections we made use of eqn. (2.21) to define a macroscopic potential Φ:

$$\dot{E}_{ij}^P \, d\Sigma_{ij} - \sum_\alpha \dot{f}_n^\alpha \, d\Sigma_h^\alpha \, v_\alpha = d\Phi \tag{5.4}$$

Substituting for $\dot{f}_h^\alpha$ using eqn. (5.3) gives

$$\dot{E}^{p}_{ij}\, d\Sigma_{ij} - \sum_{\alpha} (D + D_{ij}(n_i n_j - \tfrac{1}{3}\delta_{ij}) + D_{ijk\ell}\,\kappa_{ijk\ell} + \ldots)\, d\Sigma^{\alpha}_{h}\, v_{\alpha} = d\Phi \tag{5.5}$$

or

$$\dot{E}^{p}_{ij}\, d\Sigma_{ij} - \frac{1}{4\pi}\int_{S} (D + D_{ij}(n_i n_j - \tfrac{1}{3}\delta_{ij}) + D_{ijk\ell} + \ldots) d\Sigma^{\alpha}_{c}\, ds = d\Phi \tag{5.6}$$

We can now define a set of stress like quantities

$$\begin{aligned} \Sigma^{A} &= \frac{1}{4\pi}\int_{S} \Sigma^{\alpha}_{h}\, ds \\ \Sigma^{A}_{ij} &= \frac{1}{4\pi}\int_{S} \Sigma^{\alpha}_{h}\,(n_i n_j - \tfrac{1}{3}\delta_{ij})ds \\ \Sigma^{A}_{ijk\ell} &= \frac{1}{4\pi}\int_{S} \Sigma^{\alpha}_{h}\,\kappa_{ijk\ell}\, ds \end{aligned} \tag{5.7}$$

etc.

Eqn. (5.7) then becomes

$$\dot{E}^{p}_{ij}\, d\Sigma_{ij} - (\dot{D}\, d\Sigma^{A} + \dot{D}_{ij}\, d\Sigma^{A}_{ij} + \dot{D}_{ijk\ell}\, d\Sigma^{A}_{ijk\ell} + \ldots) = d\bar{\Phi} \tag{5.8}$$

Therefore

$$\begin{aligned} E_{ij} &= \frac{\partial\bar{\Phi}}{\partial\Sigma_{ij}} \\ \dot{D} &= -\frac{\partial\bar{\Phi}}{\partial\Sigma^{A}} \\ \dot{D}_{ij} &= -\frac{\partial\bar{\Phi}}{\partial\Sigma^{A}_{ij}} \\ \dot{D}_{ijk\ell} &= -\frac{\partial\bar{\Phi}}{\partial\Sigma^{A}_{ijk\ell}} \end{aligned} \tag{5.9}$$

etc.

Again we find the same general form of result as in the previous sections. The inelastic strain-rate and the rate of change of the state variables are derivable from a single scalar potential.

6. Damage Mechanisms in Precipitation Hardened Materials

In the situations considered in the previous sections it has been assumed that the tertiary stage of creep is a direct result of the growth of voids in the material. The nickel based superalloys tested by Dyson et al. [24] and the aluminum alloy tested by Leckie and Hayhurst [5] exhibit extensive tertiary regions, yet are found to be virtually void free until just before failure. Stevens and Flewitt [25] suggested that the steadily increasing strain-rate of the nickel alloy is a result of precipitates coarsening in the material, which thus become a less effective barrier to dislocation motion. Dyson and McLean [26] found that a model based on precipitate coarsening is unable to explain the response of these alloys and proposed that tertiary creep is a result of an increase of the mobile dislocation density with increasing strain.

Henderson and McLean [8] observed that dislocation networks form around the coherent precipitates of the nickel based superalloy IN738LC when the material creeps. They suggested that the presence of these networks aids the climb of dislocations over the particles either by acting as a source or sink for vacancies or providing a fast diffusion path for the vacancies, resulting in an increased strain rate. This mechanism has been analyzed by Ashby and Dyson [4] and by Cocks [9].

A detailed analysis of the deformation mechanism is given by Shewfelt and Brown [27] for particle strengthened materials. The essential features of the process are shown in Fig. 9. For a material to deform plastically dislocations must be able to glide along slip planes. If the material contains obstacles to dislocation motion then the dislocation must bypass them either by bowing between them, Fig. 9a, or by climbing over them, Fig. 9b. The time for a dislocation to transverse a slip plane is determined by the climbing

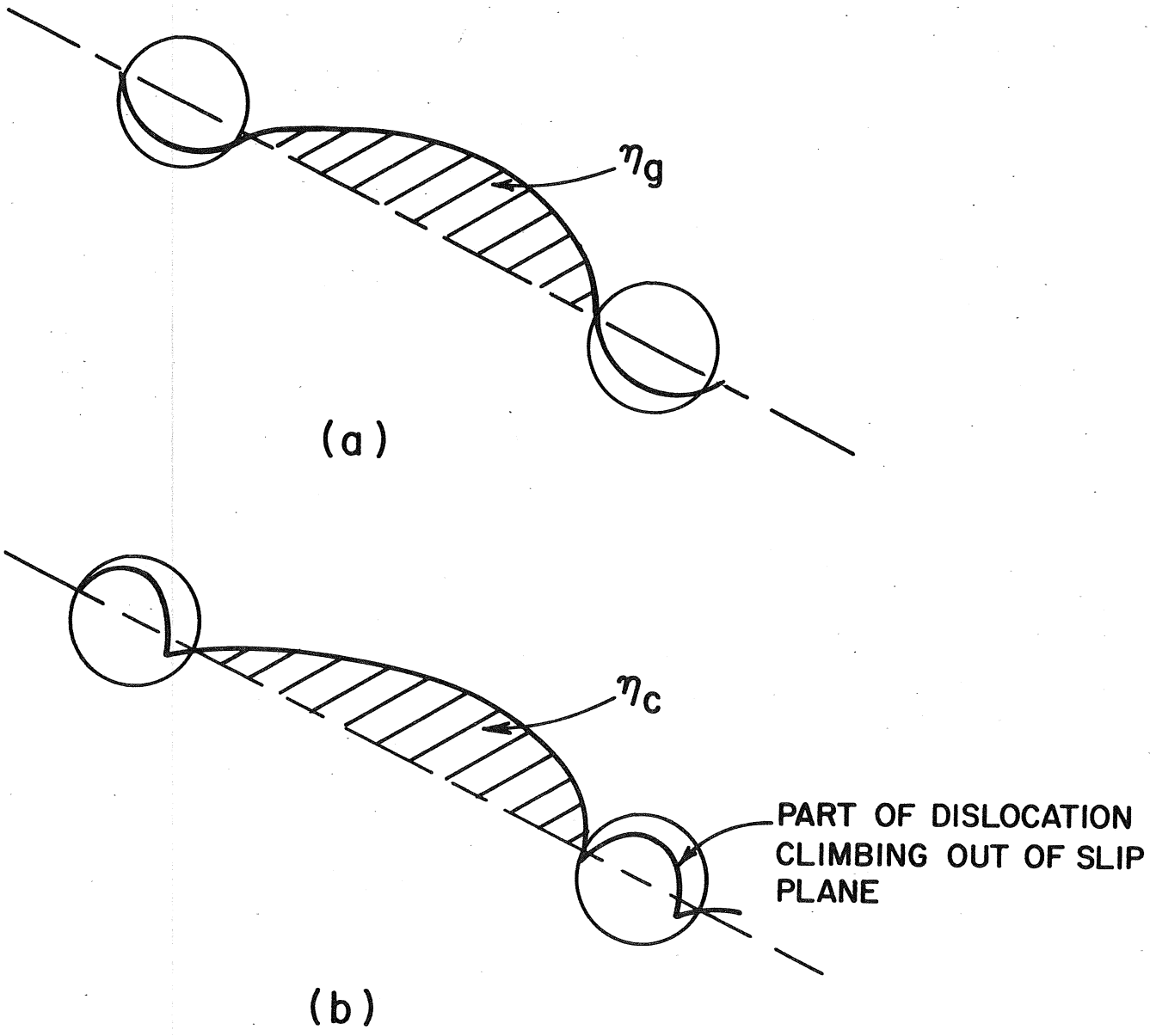

Fig. 9. (a) A section of dislocation gliding between two obstacles. (b) The section of dislocation between the two obstacles can only glide if part of it climbs over the particles.

part of the process.

Consider an element of material which sees a remote stress Σ^{α}_{ij}. Within this material dislocations move on slip planes with outward normals $\underline{n}^{\alpha}$, in the direction $\underline{s}^{\alpha}$. We can identify two families of internal state variables at a given instant in time: η_g, the area swept out by a segment of gliding dislocation, Fig. 9a; and η_c, the area swept out by a segment of dislocation in the glide plane which requires climb over an adjacent particle in order for it to move, Fig. 9b. The free energy at any instant can be found by following the procedure outlined in section 2:

$$\psi = \frac{1}{2} C_{ijk\ell} E^e_{k\ell} E^e_{ij} V + f(\eta_g) + g(\eta_c) \tag{6.1}$$

where $f(\eta_g)$ and $g(\eta_c)$ represent the free energy due to the presence of dislocation lines in the material.

Differentiating eqn. (6.1) gives

$$\dot{\psi} = \Sigma_{ij} \dot{E}^e_{ij} V + f'(\eta_g) \dot{\eta}_g + g'(\eta_c) \dot{\eta}_c \tag{6.2}$$

Substituting this into the second law (eqn. 2.6) gives

$$\Sigma_{ij} \dot{E}^p_{ij} V - f'(\eta_g) \dot{\eta}_g - g'(\eta_c) \dot{\eta}_c \geq 0 \tag{6.3}$$

Now the inelastic strain-rate, $\dot{E}^p_{ij}$ is related to $\dot{\eta}_g$ and $\dot{\eta}_c$ by (see Appendix for derivation of this expression)

$$\dot{E}^p_{ij} = (\dot{\eta}_g + \dot{\eta}_c) \frac{b}{2V} [n_i s_j + n_j s_i] \tag{6.4}$$

Combining eqns. (7.3) and (7.4) gives the rate of energy dissipation

$$[\tau b - f'(\eta_g)]\dot{\eta}_g + [\tau b - g'(\eta_c)]\dot{\eta}_c \geq 0 \tag{6.5}$$

where $\tau = \frac{\Sigma_{ij}}{2} [n_i s_j + n_j s_i]$ is the shear component of the remote stress in

the direction of slip.

To complete the thermodynamic description we need expressions for $\dot{\eta}_g$ and $\dot{\eta}_c$. Conventional theorems of dislocation glide assume that

$$\dot{\eta}_g = \dot{\eta}_g(\tau b - f'(\eta_g)) \tag{6.6}$$

When climb is required for a section of dislocation to glide Shewfelt and Brown [27] demonstrate that

$$\dot{\eta}_c = \dot{\eta}_c(\tau\ b - g'(\eta_c), \text{ geometry}) \tag{6.7}$$

where the geometric terms are functions of the size, shape and spacing of the particles and, as we shall see later, of the density of dislocation loops surrounding the particles, which is related to η_g. These expressions are of the form of eqn. (2.10), and making use of the result of eqn. (2.15), we can define potentials for each process, then

$$\Phi = \Phi_g + \Phi_c \tag{6.8}$$

where Φ_g is the potential for glide deformation and Φ_c is that for climb.

Both of the above deformation processes need to occur if the material is to deform plastically to any extent, and the two thermodynamic forces $f'(\eta_g)$ and $g'(\eta_c)$ adjust so that on average $\dot{\eta}_g = \dot{\eta}_c$. This ensures that the increase of dislocation line length during the deformation process is minimized. Cocks [9] demonstrates that if τ_o is the stress at which all the particles are bypassed by an Orowan bowing mechanism, then for a stress τ a fraction $\frac{\tau}{\tau_o}$ of the strain can be assigned to the pure gliding process and the remainder to the climb controlled process. Then on average

$$\Phi_g = \frac{\tau}{\tau_o}\Phi_c' \quad \text{and} \quad \Phi_c = (1 - \frac{\tau}{\tau_o})\Phi_c' \tag{6.9}$$

where $\Phi'_c = A(\eta_g)\ (\tau - s_c)^{n+1}$ is the potential within the volume of material where the deformation is controlled by climb. Here $A(\eta_g)$ is a kinetic constant that is a function of ηg and s_c is the maximum value of $g'(\eta_c)/b$ as a section of dislocation climbs over a particle. The functional dependence of A on η_g arises from the fact that dislocation loops form around the particles when they are bypassed by the Orowan mechanism and the presence of these loops aids the climb of the mobile dislocation. Now the potential Φ_g for glide controlled deformation is a function of $(\tau - s_g)$:

$$\Phi_g = \frac{\tau}{\tau_o} f(\tau - s_g) = \frac{\tau}{\tau_o} \Phi'_c \tag{6.10}$$

where s_g is the maximum value of $f'(\eta_g)/b$ as a dislocation bypasses a particle and the equality with $\frac{\tau}{\tau_o} \Phi'_c$ arises from the condition that the rates of η_c and η_g must balance. The rate of increase of η_g is then given by

$$\dot{\eta}_g = - \frac{\partial \Phi_g}{\partial s_g} = - \frac{\partial \Phi}{\partial s_g} \tag{6.11}$$

Eqn. (6.11) is the damage rate eqn and the strain-rate is given by

$$\dot{E}^{\alpha p}_{ij} = \frac{\partial \Phi}{\partial \Sigma^{\alpha}_{ij}}$$

where
$$\Phi = \frac{\tau}{\tau_o} f(\tau - s_g) + (1 - \frac{\tau}{\tau_o}) \frac{A(\eta_g)}{n+1} (\tau - s_c)^{n+1} \tag{6.12}$$
$$= \frac{A(\eta_g)}{(n+1)} (\tau - s_c)^{n+1}$$

In the above analysis we have assumed that there is only one slip plane operating. For the deformation of a grain in a polycrystal to be compatible more than one slip system needs to operate. So the potential, which is

expressed in terms of the local stress, is the sum of the contributions from each slip system. The macroscopic potential is then the volume average of the microscopic potentials for each grain. The stress within each grain must be in equilibrium with the applied stress, which is the only stress that appears in the macroscopic potential. In the steady state the strain-rate in each grain is the same [2,25] and all the state variables are related to each other [2], so that a single state variable theory can be used to describe the material behavior. We further assume that each grain contains the same distribution of obstacles, so that s_c for each slip system is the same. If the damage accumulates slowly, so that the strain-rate remains uniform throughout the material, the same density of loops will form around each particle. In the multiple slip situation it is this density of loops that is the damage in the material. Equation (6.12) then becomes

$$\Phi = \frac{\Sigma_e}{\Sigma_o} F(\Sigma_e - \Sigma_g) + (1 - \frac{\Sigma_e}{\Sigma_o}) \frac{A(\omega)}{n+1} (\Sigma_e - \Sigma_t)^{n+1}$$

$$= \frac{A(\omega)}{n+1} (\Sigma_e - \Sigma_t)^{n+1} \qquad (6.13)$$

and

$$\dot{E}^p_{ij} = \frac{\partial \Phi}{\partial \Sigma_{ij}} \qquad (6.14a)$$

$$\dot{\omega} = - \frac{\partial \Phi}{\partial \Sigma_g} \qquad (6.14b)$$

where Σ_e is an effective stress, Σ_t is a threshold stress related to s_c of eqn. (6.12), Σ_g is related to S_g, and ω is a measure of the density of dislocation surrounding the particles. The form of this potential reflects the fact that the overall deformation results from two processes (climb and glide controlled) which proceed at matching rates, but only the glide controlled part of the process leads to accumulation of damage in the

material.

It does not matter how the dislocations approach the particles, they will always see the same network of dislocations. In this instance the damage ω is therefore a scalar quantity.

7. Theoretical Constitutive Equations for Void Growth

In the previous sections we concentrated mainly on the structure of constitutive equations, without saying much about particular forms for these equations. In the last section however we did end up with a specific form of equation. In this section we obtain forms for these equations for two simple distributions of cavitated boundaries. These two distributions of voids represent the extremes of behavior we would expect when the damage is in the form of voids. In the next section we adopt a different approach, and try and obtain simple constitutive laws directly from the material data.

7.1 Unconstrained cavity growth

In the absence of any voids a material creeps at a rate (eqn. 3.1)

$$\dot{E}^{p}_{ij} = \frac{\partial \phi}{\partial \sigma_{ij}} \tag{7.1}$$

where $$\phi = \frac{\sigma_o \dot{\varepsilon}_o}{(n+1)} \left(\frac{\Sigma_e}{\sigma_o}\right)^{n+1}$$

We will assume that this is the strain-rate measured experimentally, so that eqn. (7.1) includes the effects of any grain-boundary sliding. When grain-boundaries slide freely the stress across the grain-boundary may not equal the resolved component of the remote stress. Analyses of the effects of grain-boundary sliding [12,28,29,30] suggest that stress normal to a given grain boundary is

$$\Sigma_n^\alpha = c\, S_{ij}\, n_i^\alpha\, n_j^\alpha + \Sigma_m \tag{7.2}$$

where S_{ij} are the remote deviatoric stresses, Σ_m the mean stress and c is constant, which is a function of the shape of the grains, that ranges from 1 to 4.

In this section we assume that the strain resulting from the growth of the voids on the grain boundaries is readily accommodated by grain-boundary sliding and the deformation of the grains, in such a way that the stress normal to the grain boundary is still given by eqn. (7.2). When void growth is controlled by grain-boundary diffusion the additional strain-rate due to the growth of the voids can be found by combining eqn. (7.2) with eqns. (3.16), (3.19) and (3.7). The macroscopic potential is then

$$\Phi = \frac{\dot{\varepsilon}_o\, \sigma_o}{(n+1)} \left(\frac{\Sigma_e}{\sigma_o}\right)^{n+1} + \sum_\alpha \frac{\Omega\, v_\alpha}{2\ell^{\alpha 3}\, \ln 1/f_h^\alpha} \left(\Sigma_n^\alpha - \Sigma_h^\alpha\, f_h^{\alpha\, -1/2}\right)^2 \tag{7.3}$$

where Σ_n^α is given by eqn. (7.2) and Σ_h^α is the associated thermodynamic internal stress. Differentiating eqn. (7.3) gives the strain rate and rate of increase of damage:

$$\dot{E}_{ij}^p = \frac{\partial \Phi}{\partial \Sigma_{ij}} = \dot{\varepsilon}_o \left(\frac{\Sigma_e}{\sigma_o}\right)^n \frac{\partial \Sigma_e}{\partial \Sigma_{ij}} + \sum_\alpha \frac{\Omega v_\alpha}{\ell^{\alpha 3}\, \ln 1/f_h^\alpha} \left(\Sigma_n^\alpha - \Sigma_h^\alpha\, f_h^{\alpha\, -1\ 2}\right) \left[C\left(\eta_i^\alpha\, \eta_j^\alpha - \frac{1}{3}\,\delta_{ij}\right) + \frac{1}{3}\,\delta_{ij}\right] \tag{7.4}$$

$$\dot{f}_h^\alpha = -\frac{1}{v_\alpha} \frac{\partial \Phi}{\partial \Sigma_h^\alpha} = \frac{\Omega}{\ell^{\alpha 3} f_h^{\alpha\, 1/2}\, \ln 1/f_h^\alpha} \left(\Sigma_n^\alpha - \Sigma_h^\alpha\, f_h^{\alpha\, -1/2}\right) \tag{7.5}$$

The last term in eqn. (7.4) represents the contributions to the strain rate from void growth, and from the additional grain-boundary sliding required to

accommodate this growth.

If, instead, the void growth is controlled by surface diffusion, the strain-rate and void growth rate can be obtained by combining eqns. (3.16), (3.27), (3.28) and (7.2); then

$$\Phi = \frac{\dot{\varepsilon}_o \sigma_o}{(n+1)} \left(\frac{\Sigma_e}{\sigma_o}\right)^{n+1} + \sum_\alpha \frac{\Delta v_\alpha f_h^{\alpha\, 1/2} \Sigma_h^\alpha}{(1 - f_h^\alpha)^3} (\Sigma_n^\alpha)^3 \tag{7.6}$$

and

$$\dot{E}_{ij}^p = \dot{\varepsilon}_o \left(\frac{\Sigma_e}{\sigma_o}\right)^n \frac{\partial \Sigma_e}{\partial \Sigma_{ij}} + \sum_\alpha \frac{3\Delta v_\alpha f_h^{\alpha\, 1/2} \Sigma_h^\alpha}{(1 - f_h^\alpha)^3} \Sigma_n^{\alpha\, 2} \left[c\left(n_i^\alpha n_j^\alpha - \tfrac{1}{3}\delta_{ij}\right) + \tfrac{1}{3}\delta_{ij}\right] \tag{7.7}$$

with

$$\dot{f}_h^\alpha = -\frac{1}{v_\alpha}\frac{\partial \Phi}{\partial \Sigma_h^\alpha} = \frac{\Delta f_h^{\alpha\, 1/2} \Sigma_h^\alpha}{(1 - f_h^\alpha)^3} (\Sigma_n^\alpha)^3 \tag{7.8}$$

8.2 Constrained cavity growth

In obtaining the potentials of eqns. (7.3) and (7.6) it was assumed that the presence of the voids does not affect the stress field within the material. For large area fractions of voids or small stresses the local strains resulting from the growth of the voids under the applied stress cannot be accommodated by grain-boundary sliding. The stresses in these regions must then relax. The limiting case is when the local stress in the vicinity of the grain boundary is much less than the applied stress. This local stress can then be ignored and the grain-boundary regions can be treated as penny-shaped cracks embedded in a creeping material (28,30,31). For non interacting cracks with no grain-boundary sliding Hutchinson shows [31]

$$\Phi = \frac{\dot{\varepsilon}_o \sigma_o}{n+1}\left(\frac{\Sigma_e}{\sigma_o}\right)^{n+1}\left\{1 + \sum_\alpha \rho^\alpha \left(\frac{\Sigma_{ij} n_i^\alpha n_j^\alpha - \Sigma_h^\alpha f_h^\alpha}{\Sigma_e}\right)^{-1/2 \; 2}\right\} \qquad (7.9)$$

where ρ^α is a measure of the density of a family of cavitated facets: $\rho \approx A_\alpha^{3/2} N^\alpha (n+1)(1+3/n)^{-1/2}$ where N^α is the number of facets with outward normals $\underline{n}_1^\alpha$ and $\underline{n}_2^\alpha$.

Differentiating Φ gives the rates strain and damage rates

$$\dot{E}_{ij}^p = \frac{\partial \Phi}{\partial \Sigma_{ij}} = \dot{\varepsilon}_o \left(\frac{\Sigma_o}{\sigma_o}\right)^n \left\{\frac{3}{2}\frac{S_{ij}}{\sigma_o} + \sum_\alpha \rho^\alpha \left[\frac{3}{2}\frac{n-1}{n+1}\frac{S_{ij}}{\Sigma_e}\left(\frac{\Sigma_{ij} n_i^\alpha n_j^\alpha - \Sigma_h^\alpha f_h^\alpha}{\Sigma_e}\right)^{-1/2 \; 2}\right.\right.$$

$$\left.\left. + \frac{2}{n+1}\left(\frac{\Sigma_{ij} n_i^\alpha n_j^\alpha - \Sigma_h^\alpha f_h^\alpha}{\Sigma_e}\right)^{-1/2} n_i^\alpha n_j^\alpha\right]\right\} \qquad (7.10)$$

$$\text{and} \quad \dot{f}_h^\alpha = -\frac{1}{v_\alpha}\frac{\partial \Phi}{\partial \Sigma_h^\alpha} = \frac{A_\alpha^{1/2}/r_h}{(1+3/n)^{1/2}}\left(\frac{\Sigma_e}{\sigma_o}\right)^{n-1}\left(\frac{\Sigma_{ij} n_i^\alpha n_j^\alpha - \Sigma_h^\alpha f_h^\alpha}{\sigma_o}\right)^{-1/2} \qquad (7.11)$$

The important result here is that the ratio of the size of the voids to the size of the grain-boundary facets plays a role in determining the rate of increase of damage. The larger the facet size, the larger the volume of material unloaded due to its presence, and the faster the creep and damage rates. Tvergaard [30] has suggested modifications to these equations to take into account the effects of grain-boundary sliding based on computations of an axisymmetric problem and the analysis of Rice [28]. The stress $\Sigma_{ij} n_i^\alpha n_j^\alpha$ is replaced by Σ_n of eqn. (7.2) and ρ^α is replaced by $\rho^{*\alpha} = C_2 \rho^\alpha$, where C_2 is a constant ranging from 1 to 200 depending on the degree of constraint imposed by the surrounding grains. The strain-rate and rate of change of internal state variables follow as before.

In the following section we analyze a simplified form of these potentials, so that we can compare the predictions with the results of multiaxial stress state experiments. We assume that the most critical damage lies on grain-boundaries which are normal to the maximum principal stress, and ignore the damage accumulating on other grain-boundaries. The consequences of this assumption are analyzed.

8. Experimental Determination of Constitutive Laws

A large body of experimental data has been collected on the fracture properties of a number of materials under both uniaxial and multiaxial states of stress. In general these experiments have been conducted at constant stress, or, when the stress has been varied, this has been done in a proportional manner. An exception to this are the experiments of Trampczynski et al. [32,33] on thin walled tubes of copper, an aluminum alloy and a nimonic. In these experiments the axial load was kept constant while the torque experienced by the tube was cycled between two prescribed limits.

First we consider the case of constant load and develop constitutive equations that can deal specifically with this situation. Then we consider the situation of non-proportional loading. In particular we concentrate on developing eqns. for copper and an aluminum alloy, which have been tested extensively by Leckie and Hayhurst [5,6] over the temperature range of 150-300°C.

8.1 General features of material behaviour at constant stress

When tested in uniaxial tension it is often found that the time to failure, t_f, and the uniaxial stress σ are related by an equation of the form

$$t_f = A\sigma^{-\nu} \tag{8.1}$$

over a range of stress, where A and ν are material constants. In most materials it is found that ν is less than the creep exponent n. For the copper tested by Leckie and Hayhurst [33] it was found that $\nu = 5.6$ and $n = 5.9$. For the aluminum alloy, however it was found that ν was greater than n, with $\nu = 10$ and $n = 9$. We explain this observation later through consideration of the strain softening mechanism of section 6.

Any constitutive equations we develop for the material behaviour, as well as reflecting the stress dependence of eqn. (8.1), must also reflect the shape of the uniaxial creep curve. Fig. 10 shows two typical creep curves for aluminum and copper. The important characteristic of these curves is the value of the quantity λ (the creep damage tolerance [4]):

$$\lambda = \frac{\varepsilon_f}{\dot{\varepsilon}_{ss}\, t_f} \tag{8.2}$$

which is a measure of the materials ability to redistribute stress in a structural sitution. $\lambda \approx 10$ for aluminum and $\lambda \approx 4.0$ for copper.

The results of multiaxial stress state tests are conveniently plotted as isochronous surfaces in stress space, Fig. 11. These surfaces connect points which give the same time to failure. Fig. 11 shows the isochronous surfaces found experimentally for copper and the aluminum alloy [5]. Failure in copper is a function of the maximum principal stress, while aluminum fails according to an effective stress criterion.

When analyzing the deformation of a structure subjected to proportional loading it is found that a single state variable theory adequately describes

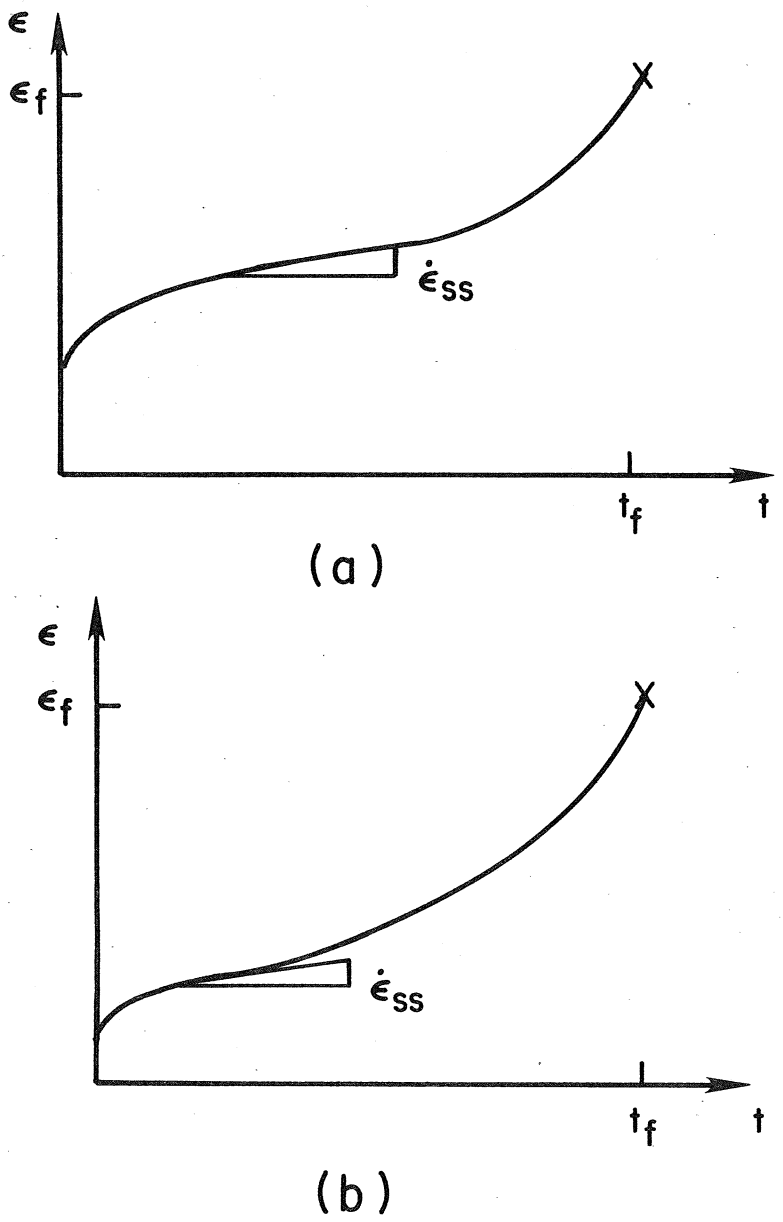

Fig. 10. Uniaxial creep curves for (a) copper and (b) an aluminum alloy.

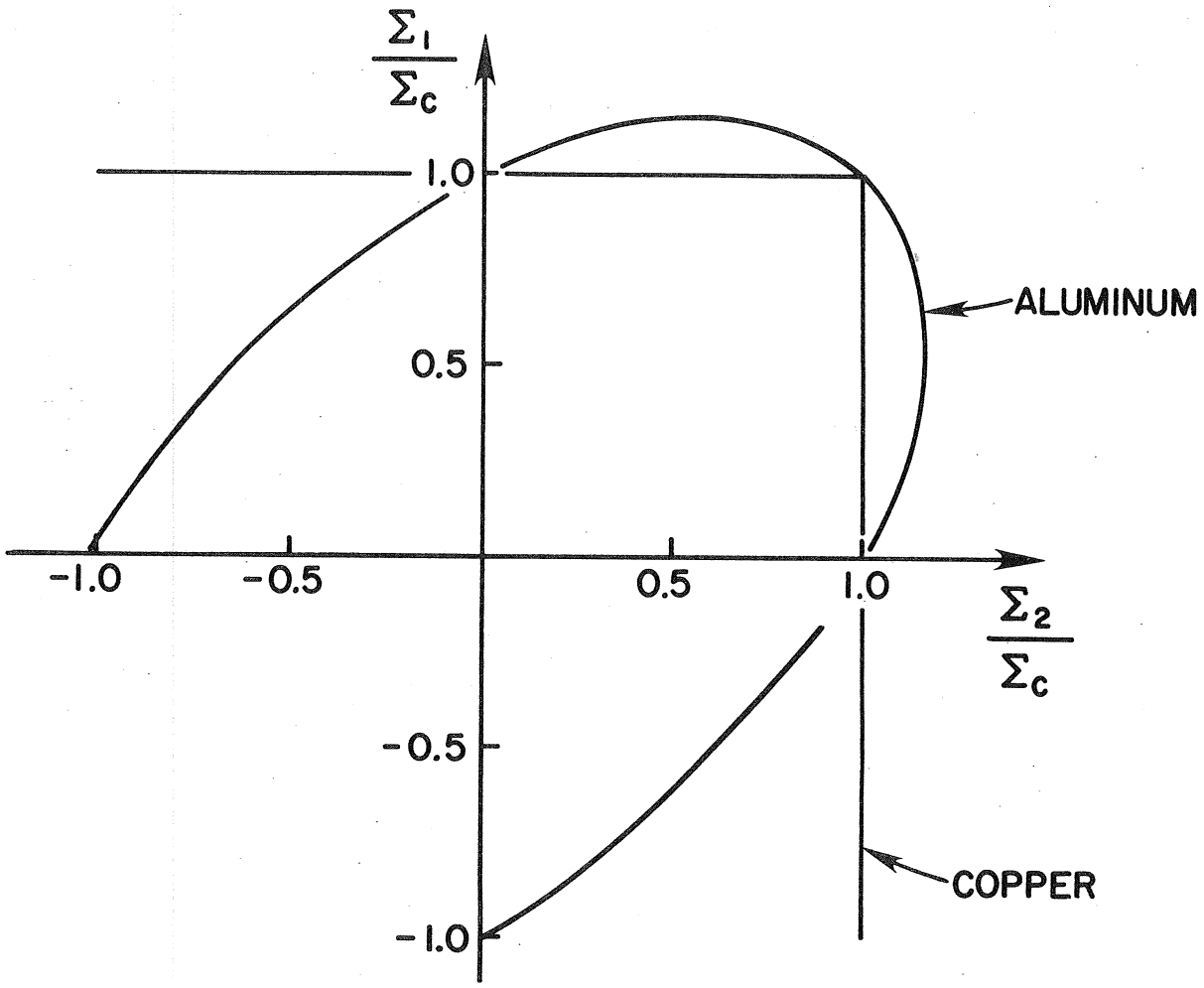

Fig. 11. Isochronous surfaces in plane stress space for copper and aluminum.

the response of the structure [3]. It is also found that a single state variable theory gives good predictions of the time to failure of structures subjected to constant and moderate levels of cyclic loading [5]. In section 8.2 we reduce each of the void growth models of section 7 to a single state variable theory by assuming that most of the void damage lies on grain-boundaries which are normal to the maximum principal stress. We obtain isochronous surfaces for each model and compare them with the experimental surfaces for copper and aluminum.

8.2 Theoretical single state variable theories of creep damage

In section 6 we developed a single state variable theory for the creep deformation of a material which strain softens, where the damage is represented by a scalar quantity, eqns. (6.13) and (6.14). For conditions of constant stress eqn. (6.14b) can be integrated to give the time to failure t_f

$$\int_0^{\omega_f} \frac{d\omega}{f(\omega)} = A_o \, (\Sigma_o - \Sigma_t)^n \, \frac{\Sigma_e}{\Sigma_o} \int_0^{t_f} dt \tag{8.3}$$

where ω_f is the value of ω at failure. If $\Sigma_e = \frac{3}{2} S_{ij} S_{ij}$ is the von Mises effective stress then failure occurs in a uniaxial test conducted at constant stress Σ_c after a time

$$t_f = \int_0^{\omega_f} \frac{d\omega}{f(\omega)} \Big/ A_o \, (\Sigma_c - \Sigma_t)^n \, \frac{\Sigma_c}{\Sigma_o} \tag{8.4}$$

Failure occurs in the multiaxial test after the same time if

$$(\Sigma_e - \Sigma_t)^n \, \Sigma_e = (\Sigma_c - \Sigma_t)^n \, \Sigma_c$$

i.e., if

$$\frac{\Sigma_e}{\Sigma_c} = 1 \tag{8.5}$$

This equation represents the shape of the isochronous surface in stress space, which, in principal plane stress space, is simply a von Mises ellipse, Fig. 12. The stress dependence of the time to failure is given by eqn. (8.4)

$$t_f \propto \frac{1}{(\Sigma_c - \Sigma_t)^n \Sigma_c} \tag{8.6}$$

The uniaxial creep curve can be obtained by integrating eqn. (8.11). The shape of this curve and the value of λ depend on the exact form of the function $f(\omega)$. The way to choose $f(\omega)$ would be to fit the shape of the creep curve. Ashby and Dyson [4] show that for this mechanism one would expect large values of λ, $\lambda > 10$.

Next we turn our attention to the theoretical models of void growth. We assume in each case that only one family of grain boundaries are cavitated, those which lie on the boundaries normal to the maximum principal stress. Eqns. (7.4) and (7.5) for void growth by grain-boundary diffusion then become

$$\dot{E}^p_{ij} = \varepsilon_o \left(\frac{\Sigma_e}{\sigma_o}\right)^n \frac{\partial \Sigma_e}{\partial \Sigma_{ij}} + \frac{\Omega v}{\ell n\ 1/f_h} (\Sigma^*_I - \Sigma_h f_h^{-1/2}) \left[C(n_i n_j - \tfrac{1}{3}\delta_{ij}) + \tfrac{1}{3}\delta_{ij}\right]$$

$$\dot{f}_h = \frac{\Omega}{\ell^{\alpha 3} f_h^{1/2} \ell n\ 1/f_h} (\Sigma^*_I - \Sigma_h f_h^{-1/2}) \tag{8.7}$$

where

$$\Sigma^*_I = c\, S_{ij}\, n_i\, n_j + \Sigma_m$$

and $\underline{n}$ is in the direction of the maximum principal stress Σ_I. In general $\Sigma_h f_h^{-1/2} \ll \Sigma^*_I$ so that eqn. (8.7) simplifies to

$$\dot{f}_h = \frac{\Omega}{\ell^{\alpha 3} f_h^{1/2} \ell n\ 1/f_h} \Sigma^*_I \tag{8.8}$$

The time to failure can be found by integrating eqn. (8.8) between the limits

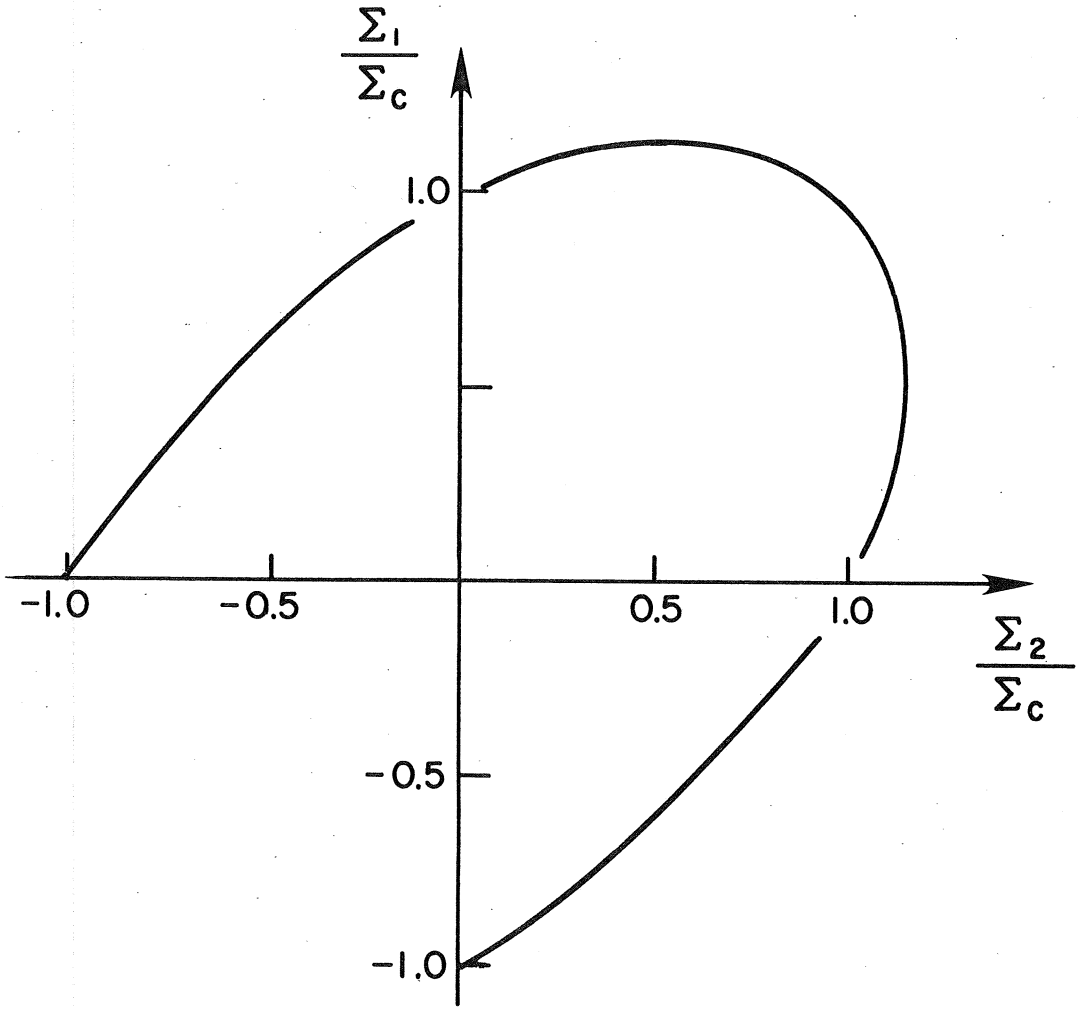

Fig. 12. Isochronous surface for strain-softening mechanism.

$$f_h = f_i \quad \text{at} \quad t = 0$$
$$f_h = f_c \quad \text{at} \quad t = t_f \tag{8.9}$$

giving
$$\int_{f_i}^{f_c} f_h^{1/2} \ln 1/f_h \, df_h = \frac{\Omega}{\ell^3} \Sigma_I^* \, t_f \tag{8.10}$$

The time to failure in uniaxial tension test is given by setting $\Sigma_I^* = \frac{1}{3}(1 + 2c)\Sigma_c$ in eqn. (8.10), and the shape of the isochronous surface is then represented by

$$\frac{3\Sigma_I^*}{(1 + 2c)\Sigma_c} = 1 \tag{8.11}$$

Isochronous surfaces for c = 1 and c = 1.5 are shown in Fig. 13. The stress dependence of the time to failure is now

$$t_f \propto \frac{1}{\Sigma} \tag{8.12}$$

When void growth is controlled by surface diffusion eqns. (8.7) and (8.8) become

$$\dot{E}_{ij}^p = \varepsilon_o \left(\frac{\Sigma_e}{\sigma_o}\right)^n \frac{\partial \Sigma_e}{\partial \Sigma_{ij}} + 3\Delta \, \frac{f_h^{1/2} \, \Sigma_h \, \Sigma_I^{*2}}{(1 - f_h)^3} \left[C\left(n_i \, n_j - \frac{1}{3}\delta_{ij}\right) + \frac{1}{3}\delta_{ij}\right] \tag{8.13}$$

$$\dot{f}_h = \frac{\Delta \, f_h^{1/2} \, \Sigma_h \, \Sigma_I^{*3}}{(1 - f_h)^3} \tag{8.14}$$

Integration of eqn. (8.14) between the limits of eqn. (8.9) gives the same isochronous failure surface as for grain-boundary diffusion controlled growth, eqn. (8.11), but the stress dependence of the time to failure is now

$$t_f \propto \frac{1}{\Sigma^3} \tag{8.15}$$

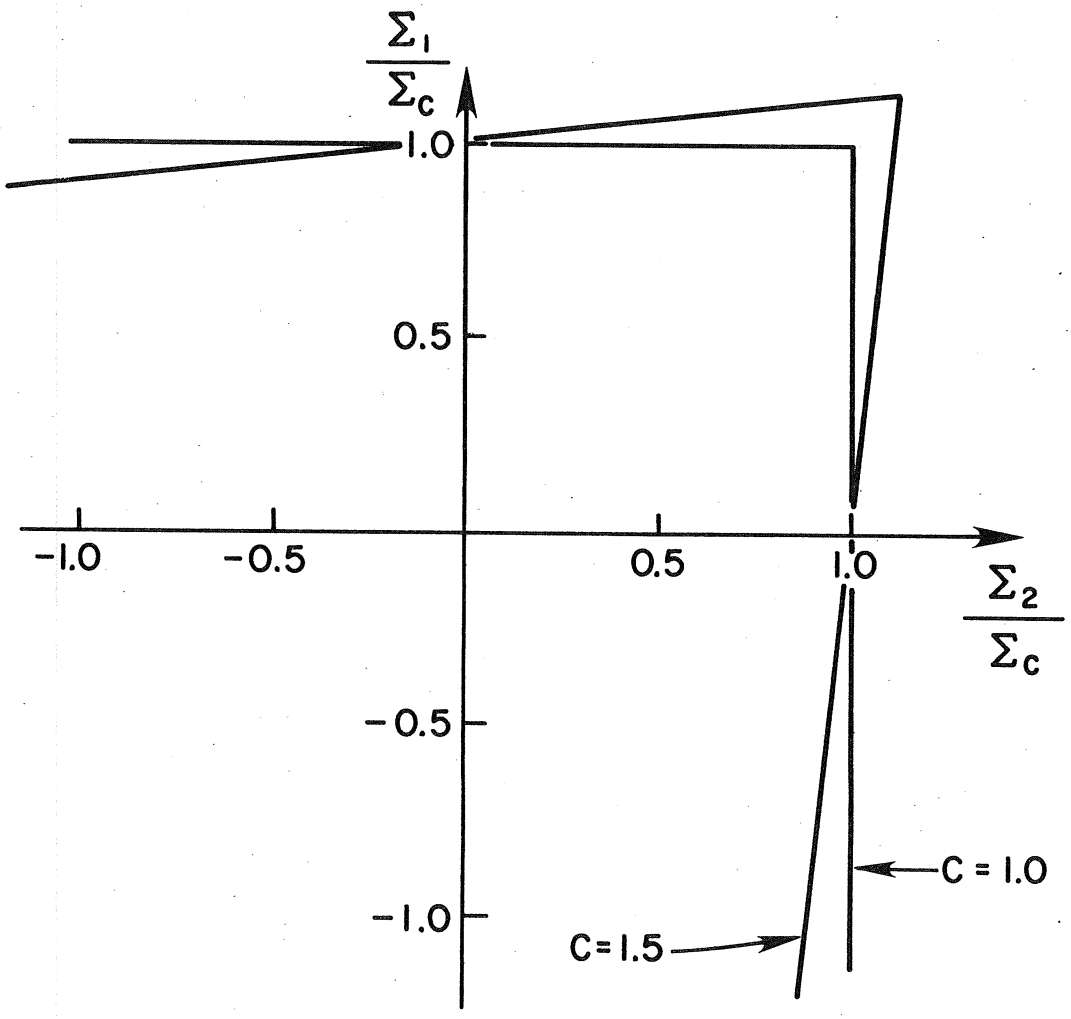

Fig. 13. Isochronous surfaces for unconstrained void growth for two values of c.

In each of these situations where void growth is unconstrained the first term in the expression for the strain-rate (eqns. (8.6) and (8.13)) dominate and there is very little tertiary creep, so $\lambda \approx 1$.

For constrained cavity growth the constitutive relationships for one family of cavitated boundaries becomes

$$\dot{E}^p_{ij} = \dot{\varepsilon}_o \left(\frac{\Sigma_e}{\sigma_o}\right)^n \left\{\frac{3}{2}\frac{S_{ij}}{\sigma_o} + \rho\left[\frac{3}{2}\frac{n-1}{n+1}\frac{S_{ij}}{\Sigma_e}\left(\frac{\Sigma_I - \Sigma_h f_h^{-1/2}}{\Sigma_e}\right)^2 + \frac{2}{n+1}\left(\frac{\Sigma_I - \Sigma_h f_h^{-1/2}}{\Sigma_e}\right) n_i n_j\right]\right. \tag{8.16}$$

$$\dot{f}_h = \frac{2\rho}{f_h^{1/2}(n+1)}\left(\frac{\Sigma_e}{\sigma_o}\right)^{n-1}\left(\frac{\Sigma_I - \Sigma_h f_h^{-1/2}}{\sigma_o}\right) \tag{8.17}$$

where $\Sigma_I = \Sigma_{ij}\, n_i\, n_j$ is the maximum principal stress. Again if $\Sigma_I >> \Sigma_h f_h^{-1/2}$ eqn. (8.17) can be integrated between the limits of eqn. (8.9) to give the time to failure

$$\int_{f_i}^{f_c} f_h^{1/2}\, df_h = \frac{2\rho}{n+1}\left(\frac{\Sigma_e}{\sigma_o}\right)^{n-1}\frac{\Sigma_I}{\sigma_o}\int_0^{t_f} dt \tag{8.18}$$

In uniaxial tension

$$t_f = \int_{f_i}^{f_c} f_h^{1/2}\, df_h \,\frac{n+1}{2\rho} \Big/ \left(\frac{\Sigma_c}{\sigma_o}\right)^n \tag{8.19}$$

and the shape of the isochronous surface is

$$\left(\frac{\Sigma_e}{\Sigma_c}\right)^{n-1}\frac{\Sigma_I}{\Sigma_c} = 1 \tag{8.20}$$

A surface for n = 5 is shown in Fig. 14. The stress dependence of the time to failure is

$$t_f \propto \frac{1}{\Sigma^n} \tag{8.21}$$

In this instance the value of f_h does not appear in the expression for the strain-rate (eqn. (8.16)), so the material creeps at the same rate up to the instant of failure, and $\lambda = 1$.

8.3 Constitutive equations for an aluminum alloy and copper

In section 8.2 we examined the experimental data available on an aluminum alloy and copper and in the last sub-section we examined the prediction of a number of simple constitutive relationships which resulted from our analysis of the damaging mechanisms. The question now is "do any of these equations adequately describe the response of these materials?"

The predictions of the strain-softening model are consistent with the behaviour of aluminum. The isochronous surface in each case is a von Mises ellipse and the value of λ is quite large. The stress dependence of the time to failure is slightly different, but over a small range of stress a power-law relationship gives a good fit to the strain rate data:

$$\dot{E}^p_{ij} = f(\omega)\ \varepsilon_o \left(\frac{\Sigma_e}{\sigma_o}\right)^n \frac{\partial \Sigma_e}{\partial \Sigma_{ij}}$$

$$\text{then} \qquad \dot{\omega} = f(\omega)\ \varepsilon_o \left(\frac{\Sigma_e}{\sigma_o}\right)^{n+1} \tag{8.22}$$

$$\text{and} \qquad t_f \propto \frac{1}{\Sigma^{n+1}}$$

Therefore $\nu = n + 1$, which is consistent with the experimental observation on aluminum, when it was found that $\nu = 10$ and $n = 9$. There appears to be ample

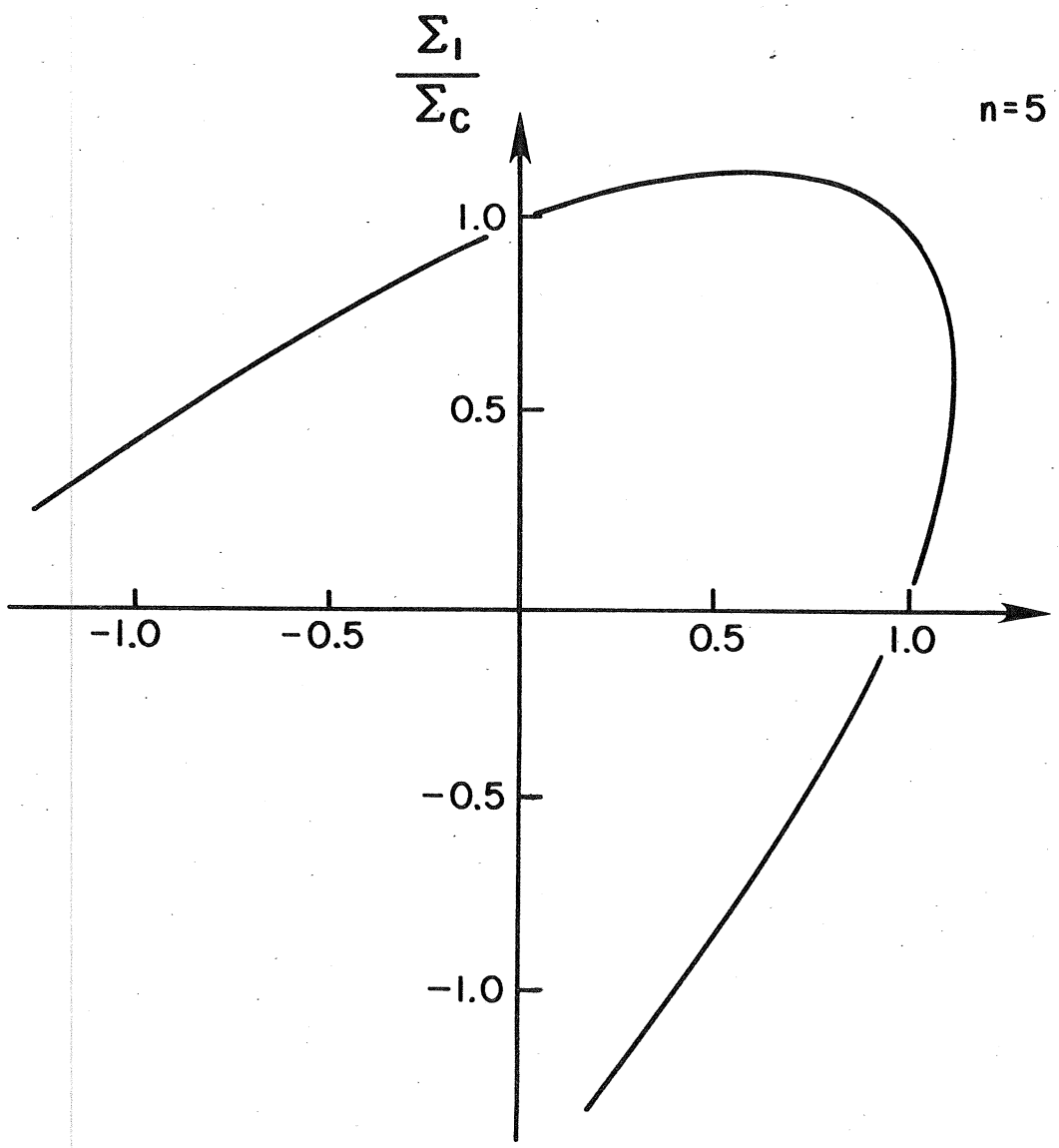

Fig. 14. Isochronous surface for constrained void growth when n = 5.

experimental evidence to support the predictions of the strain-softening mechanism. In the next sub-section on non-proportional loading we find further evidence for the applicability of this mechanism.

The isochronous failure surface for copper, Fig. 11, is the same as that for unconstrained diffusive growth with c = 1, Fig. 11 but the stress dependence of the time to failure, $\nu = 5.6$ as opposed to 1 or 3, and the creep ductility, $\lambda = 4.0$ instead of 1, are completely different. The stress dependence of the time to failure is similar to that for constrained cavity growth, $n \approx \nu$, but the shape of the isochronous surface is completely different and the prediction of the creep ductility λ is again too small.

These discrepancies are due, in part, to the fact that we have not included nucleation in our constitutive relationships. Also, for failure to occur more than one family of grain-boundaries must fail. Metallographic examination of copper specimens before final failure reveals the existence of a number of grain-boundary fissures, the number of which increases as the failure time is approached. Thus the number of crack-like features increases with time. We could analyze this situation using the potential form of section 4 with a large number of state variables. However, we would like to describe the behaviour in such a way that we need only use a single state variable.

When the voids are small there is not much accumulation of strain as they grow, there is little contribution to the macroscopic strain and their growth is essentially unconstrained. But as they get bigger the local strain-rate increases and the growth can become constrained, or the voids can link to form a crack. In either case we can analyze the behaviour as if a crack were present. When a crack-like feature forms the stress locally is relaxed and this can have a strong influence on the overall creep rate. If we assume that

these cracks all lie on grain-boundaries which are nearly normal to the maximum principal stress then we can use eqn. (8.16) for the creep rate, where ρ is a measure of the volume fraction of crack-like features, which increases as the material creeps, and is now our measure of damage in the material. The problem now becomes one of determining the rate of increase of ρ.

If, as before, we consider proportional loading and ignore the effects of rotation of material elements, we can obtain an expression for the rate of increase of ρ. First consider what happens on a given grain-boundary as the material creeps. The rate of growth of voids on the grain-boundary is given by eqn. (7.5):

$$\dot{f}_h^\alpha = \ell^{\alpha 3} \frac{\Omega}{\ell^{\alpha 3} f_h^{\alpha 1/2} \ell n\, 1/f_h^\alpha} \Sigma_n \tag{8.23}$$

where Σ_n is the stress normal to the grain-boundary. If the outward normal to this boundary makes a small angle θ with the direction of maximum principal stress, Fig. 15 then to first order

$$\Sigma_n = \Sigma_I(1 - \theta^2) + \left(\frac{\Sigma_{II} + \Sigma_{III}}{2}\right)\theta^2 \tag{8.24}$$

where Σ_{II} and Σ_{III} are the other two principal stresses. For final failure to occur all boundaries with $\theta < \bar{\theta}$ must fail where $\bar{\theta}$ is a material property. From eqn. (8.23) and (8.24) we see that damage accumulates fastest on the grain-boundaries which lie normal to the maximum principal stress. When these boundaries fail the stress is redistributed onto other parts of the material, so that the stress increases in the unfailed parts of the material.

Initially the strain-rate is given by

$$\dot{E}^p_{ij} = \dot{\varepsilon}_o \left(\frac{\Sigma_e}{\sigma_o}\right)^n \frac{\partial \Sigma_e}{\partial \Sigma_{ij}} \tag{8.25}$$

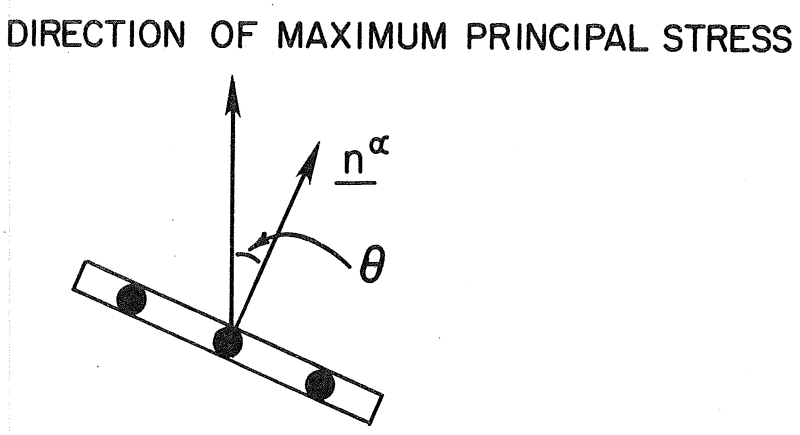

Fig. 15. The outward normal to the grain boundary makes an angle θ with the direction of maximum principal stress.

there are no grain-boundary cracks, and $\rho = 0$. The time for the formation of the first cracks can be found by integrating eqn. (8.23), with $\Sigma_n = \Sigma_I$, between the limits of eqn. (8.9); where we now interpret f_c as the value of f_h at which constraint effects become significant or the point where the voids coalesce to form a physical crack:

$$\int_{f_i}^{f_c} f_h^{1/2} \ln 1/f_h \, df_h = \frac{\Omega}{\ell^3} \Sigma_I \int_0^{t_i} dt \tag{8.26}$$

We saw in section 3 that we could choose any function of f_h or f_v to represent the damage. It is convenient at this stage to define the damage as

$$\psi = \int_{f_i}^{f_h} f_h^{1/2} \ln 1/f_h \, df_h \tag{8.27}$$

Then eqn. (8.26) becomes

$$\int_0^{\psi_c} d\psi = \frac{\Omega}{\ell^3} \Sigma_I \int_0^{t_i} dt$$

and

$$t_i = \frac{\psi_c \, \ell^3}{\Omega \, \Sigma_I} \tag{8.28}$$

For loading times in excess of t_i the damage, in the form of cracks, spreads to grain-boundaries with larger values of θ. The density of cracks is then directly related to the value of $\theta = \theta_c$ at which cracks have just nucleated. So that

$$\theta_c = B\rho \tag{8.29}$$

where B is a constant.

As ρ increases Σ_I in the uncracked material increase so that

$$\Sigma_I^* = \Sigma_I^* (\Sigma_I, \rho), \tag{8.30}$$

where the * signifies a local stress, but the stresses Σ_{II} and Σ_{III} remain the same.

The time, t, at which a crack just nucleates on boundaries with $\theta = \theta_c$ can be found by combining eqns. (8.23), (8.24) and (8.27) and integrating between the limits $\psi = 0$ at $t = 0$ and $\psi = \psi_c$ at $t = t$. Then

$$\psi_c = \frac{\Omega}{\ell^3} \int_0^t \left(\Sigma_I^* (1 - \theta_c^2) + \left(\frac{\Sigma_{II} + \Sigma_{III}}{2}\right) \theta_c^2\right) dt \tag{8.31}$$

where Σ_I^* is a function of ρ, which is a function of t. For a grain-boundary with $\theta = \theta_c + \Delta\theta$, $\psi = \psi_c - \Delta\psi$ after a time t, where

$$\psi_c - \Delta\psi = \frac{\Omega}{\ell^3} \int_0^t \left\{\Sigma_I^* (1 - \theta_c^2 - 2\theta_c \Delta\theta) + \left(\frac{\Sigma_{II} + \Sigma_{III}}{2}\right) (\theta_c^2 + 2\theta_c \Delta\theta)\right\} dt \tag{8.32}$$

Combining eqns. (8.31) and (8.32) we find

$$\Delta\psi = \frac{\Omega}{\ell^3} \int_0^t \left\{\Sigma_I^* 2\theta_c \Delta\theta - \left(\frac{\Sigma_{II} + \Sigma_{III}}{2}\right) 2\theta_c \Delta\theta\right\} dt \tag{8.33}$$

On the boundaries for which $\theta = \theta_c + \Delta\theta$, failure occurs after an additional time Δt, where

$$\Delta\psi = \frac{\Omega}{\ell^3} \left[\Sigma_I^* (1 - \theta_c^2) + \left(\frac{\Sigma_{II} + \Sigma_{III}}{2}\right) \theta_c^2\right] \Delta t \tag{8.34}$$

Combining eqns. (8.30), (8.31), (8.33) and (8.34) we find

$$\frac{\Delta\theta}{\Delta t} = \frac{\left[\Sigma_I^*(1 - \theta_c^2) + \dfrac{(\Sigma_{II} + \Sigma_{III})}{2} \theta_c^2\right] (1 - \theta_c^2)}{2\theta_c \left[\dfrac{\psi_c \ell^3}{\Omega} - \dfrac{\Sigma_{II} + \Sigma_{III}}{2}\right]} \tag{8.35}$$

and making use of eqn. (8.29) we obtain the rate of increase of damage

$$\frac{d\rho}{dt} = \frac{\Sigma_I^*(1 - B^2\rho^2) + \frac{(\Sigma_{II} + \Sigma_{III})}{2} B^2\rho^2}{2B^2\rho \left[\frac{\psi_c \ell^3}{\Omega} - \frac{\Sigma_{II} + \Sigma_{III}}{2}\right]} (1 - B^2\rho^2) \qquad (8.36)$$

where it should be remembered that Σ_I^* is also a function of ρ. The predictions of this model, and the modifications required when rotations occur are examined elsewhere [34]. Now the damage has a stronger influence on the strain-rate of the material and there is a more extensive, and more realistic, tertiary stage of creep. It should be noted however, that the times to failure obtained from this model are not too different from the unconstrained situation with one set of damaged planes, but the important modification is the more detailed description of the creep curve, particularly the tertiary stage. The stress dependence of the time to failure is still, however,

$$t_f \propto \frac{1}{\Sigma}$$

It would appear that higher values of ν require the inclusion of the nucleation process in the constitutive law, although a value of $\nu = 3$ is obtained when the growth of damage on the grain-boundaries is controlled by surface diffusion. The effects of including nucleation are examined in [34]. The analysis of section 4 demonstrates that the nucleation of cavities is driven by the stress normal to the grain-boundary. The rate of growth of damage in the material then varies in a nonlinear manner with stress [19,22]. Cocks [22] shows how the overall damage on a grain-boundary can, in certain instances, grow at a rate proportional to Σ_I^n, where n is the creep exponent. This mechanism, combined with the above analysis, appears to have the potential of explaining the experimental observations made on copper.

8.4 Non-proportional cyclic loading

In the previous sub-sections we concentrated primarily on proportional, or constant, loading situations where we could describe the material behaviour in terms of a single damage parameter. In some structural situations components experience non-proportional cyclic loading. Examples of this can be found in a number of components of the Liquid Metal Cooled Fast Breeder Nuclear Reactor which experiences cyclic thermal loading as the reactor is shut down and started up. It is therefore important to understand how a material behaves under these types of loading conditions.

Trampczynski et al. [32,33] have performed non-proportional cyclic loading experiments on thin walled tubes of copper and aluminum. In these experiments the axial stress was maintained constant while the shear stress was cycled between $\pm \tau$. The stress levels were chosen such that the direction of maximum principal stress rotated through 32°.

In the tests on the aluminum alloy it was found that the magnitude of the components of strain-rate were the same before and after the reversal. It was also found that the time to failure was the same as when the stress-state was held constant for the entire life. These results suggest that the damage in the aluminum can be treated as a scalar quantity. This conclusion is again consistent with the predictions of the strain softening mechanism.

In tests on copper it was found that the magnitude of the strain-rates decreased after a single reversal of stress and the life was increased by a factor of 2 over that of a constant stress test. Metallographic examination of the failed specimen revealed that one set of damage grew at one end of the cycle and another set at the other extreme. The fact that the time to failure in the cyclic test is twice that in the static test indicates that there is no interaction between these two sets of damage. Two state variables are now

needed in the constitutive law and the strain-rate potential becomes (eqn. 7.9)

$$\Phi = \frac{\varepsilon_o \sigma_o}{n+1}\left(\frac{\Sigma_e}{\sigma_o}\right)^{n+1}\left\{1 + \rho_1\left(\frac{\Sigma_{ij} n_i^1 n_j^1}{\Sigma_e}\right)^2 + \rho_2\left(\frac{\Sigma_{ij} n_i^2 n_j^2}{\Sigma_e}\right)^2\right\}$$

Evolution laws for each damage measure (ρ_1 and ρ_2) must be developed as in the previous subsection. When the material is loaded so that $\Sigma_{ij}\, n_i^1\, n_j^1$ is the maximum principal stress damage will accumulate on the planes nearly normal to $\underline{n}^1$, and ρ_1 will increase as ρ_2 remains equal to zero. When the stress system is rotated so that $\Sigma_{ij}\, n_i^2\, n_j^2$ is the maximum principal stress, damage will accumulate on boundaries nearly normal to $\underline{n}^2$, while ρ_1 remains constant. Immediately after the reversal, when $\rho_2 = 0$, the magnitude of $\Sigma_{ij}\, n_i^1\, n_j^1$ decreases in eqn. (8.37) and we would expect the magnitude of the strain-rates to decrease, although the presence of this damage does effect what these strain-rates are.

9. Life Bounds for Creeping Materials

When the damage in the material is in the form of dislocation loops, or even in some situations where it is in the form of voids, the damage rate equation can be written in the form

$$\dot{\omega} = f(\omega)\, \chi(\sigma_{ij}) \tag{9.1}$$

where $f(\omega)$ is a function of the damage ω and $\chi(\sigma)$ is a function of stress. For damage growth rates in the form of eqn. (9.1) it is possible to extend the results of Ponter [35] to obtain upper bounds on the life of a component for situations of constant and cyclic loading. First we obtain bounds when the load remains constant and then in section 9.2 we examine cyclic loading.

9.1 Bounds for Constant Applied Load

As in section 8.3 a convenient measure of damage in these situations is

$$\psi = \int_{\omega_i}^{\omega} \frac{d\omega}{f(\omega)}$$

where ω_i is the initial damage

then
$$\dot{\psi} = \frac{\dot{\omega}}{f(\omega)} \tag{9.2}$$

and eqn. (9.1) becomes

$$\dot{\psi} = \chi(\sigma_{ij}) \tag{9.3}$$

Now consider a structure subjected to a constant load P, Fig. 16, then as an element of material deforms and becomes damaged the stress it experiences changes. If $f(\omega)$ is a monotonically increasing function of ω then when the structure fails after a time t_f.

$$\int_0^{t_f} \dot{\psi}\, dt \leqslant \psi_c \tag{9.4}$$

where ψ_c is the value of ψ when an element of material fails. Integrating eqn. (9.3) from t = 0 to t = t_f and integrating over the volume gives

$$\int_V \int_o^{t_f} \chi(\sigma_{ij})\, dt\, dV \leqslant \psi_c\, V \tag{9.5}$$

A further bound on the l.h.s of eqn. (9.5) can be obtained by considering the same structure composed of a model material. Here we consider two such model materials.

9.1.1 Model creeping material

Consider a material which creeps according to the relationship

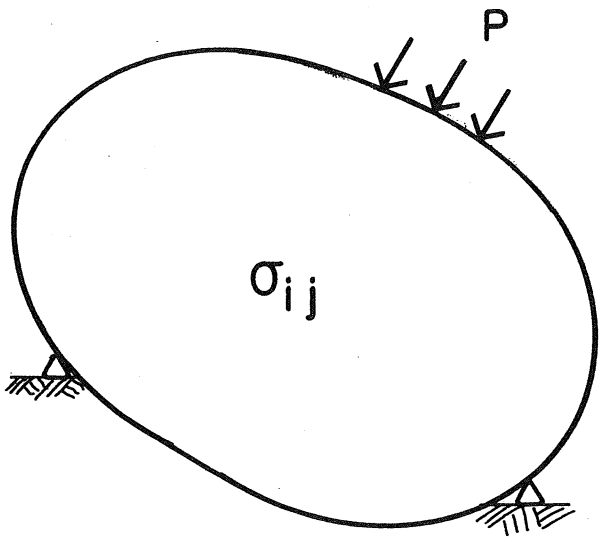

Fig. 16 Structure subjected to a constant load P fails after a time t_f.

$$\dot{\varepsilon}^{p}_{ij} = \frac{\partial \chi(\sigma_{ij})}{\partial \sigma_{ij}} \tag{9.6}$$

where, we further assume that $\chi(\sigma_{ij})$ is a convex function of stress. Then if σ^{1}_{ij} and σ^{2}_{ij} are two arbitrary stress states the convexity condition is

$$(\sigma^{1}_{ij} - \sigma^{2}_{ij}) \frac{\partial \chi(\sigma^{1}_{ij})}{\partial \sigma^{1}_{ij}} + \chi(\sigma^{2}_{ij}) - \chi(\sigma^{1}_{ij}) \geq 0 \tag{9.7}$$

If we identify σ^{2}_{ij} with the actual stress field in the material, σ_{ij}, and σ^{1}_{ij} with the solution for the model material, σ^{s}_{ij} integrating eqn. (9.7) between $t = 0$ and $t = t_f$ and then over the volume gives

$$\int_V \int_0^{t_f} \chi(\sigma_{ij})\, dt\, dV \geq \int_V \int_0^{t_f} \chi(\sigma^{s}_{ij})\, dt\, dV = \int_v \chi(\sigma^{s}_{ij})\, dV\, t_f \tag{9.8}$$

since both σ_{ij} and σ^{s}_{ij} are in equilibrium with the same load P. Substituting eqn. (9.8) into eqn. (9.5) gives

$$t_f \leq \frac{\psi_c V}{\int_V \chi(\sigma^{s}_{ij})\, dV} \tag{9.9}$$

9.1.2 Perfectly plastic material model

Now consider a perfectly plastic material with a yield surface given by an equation of the form

$$\chi(\sigma_{ij}) - \chi_c = 0 \tag{9.10}$$

where χ_c is a material constant equivalent to the yield stress. The value of χ_c is chosen such that a structure composed of the model material collapses at the applied load P. The inelastic strain-rate is given by the associated flow rule

$$\dot{\varepsilon}^{p}_{ij} = \dot{\mu} \frac{\partial \chi(\sigma_{ij})}{\partial \sigma_{ij}} \tag{9.11}$$

where $\dot{\mu}$ is a plastic multiplier.

Multiplying both sides of eqn. (9.3) by $\dot{\mu}$, integrating over the life and the volume we obtain, after noting eqn. (9.4):

$$\int_V \int_o^{t_f} \dot{\mu}\, \chi(\sigma_{ij})\, dt\, dV \leqslant \phi_c \int_V \dot{\mu}\, dV \tag{9.12}$$

Similarly eqn. (9.7) can be multiplied through by $\dot{\mu}$, integrated between $t = 0$ and $t = t_f$ and, after setting σ^1_{ij} to the stress field at the limit load for the perfectly plastic material and σ^2_{ij} to the stress field in the real material, integrated over the volume to give

$$\int_V \int_o^{t_f} (\sigma^1_{ij} - \sigma^2_{ij})\, \dot{\varepsilon}^{pl}_{ij}\, dt\, dv + \int_V \int_o^{t_f} \dot{\mu}\, \chi(\sigma^2_{ij})\, dt\, dV$$

$$- \int_V \int_o^{t_f} \dot{\mu}\, \chi(\sigma^1_{ij})\, dt\, dV \geqslant 0 \tag{9.13}$$

where $\dot{\varepsilon}^{pl}_{ij}$ is the strain-rate under a stress σ^1_{ij}.

The stress fields σ^1_{ij} and σ^2_{ij} are in equilibrium with the same load P_i and, for the model material, plastic flow can only occur when $\chi(\sigma^1_{ij}) = \chi_c$. Equation (9.12) then becomes

$$\int_V \int_o^{t_f} \dot{\mu}\, \chi(\sigma^2_{ij})\, dt\, dV \geqslant \chi_c\, t_f \int_V \dot{\mu}\, dV \tag{9.14}$$

Substituting this into eqn. (9.12) we obtain

$$t_f \leqslant \frac{\phi_c}{\chi_c} \tag{9.15}$$

If it is not convenient to obtain the exact limit load for the model material

the above bound applies when an upper bound to the unit load is obtained. Then, if P is an upper bound to the limit load for a given yield function $\overline{\chi}_c$, and is the exact solution for χ_c:

$$\overline{\chi}_c \leqslant \chi_c$$

and eqn. (9.15) becomes

$$t_f \leqslant \frac{\phi_f}{\chi_c} \tag{9.16}$$

9.2 Cyclic Loading Bounds

For situations where the cycle times are large compared to a characteristic time for stress redistribution the results of the last section can be readily extended.

Consider the global damage rate

$$\dot{\Psi} = \int_V \dot{\phi}\, dV = \int_V \chi(\sigma_{ij})\, dV \tag{9.17}$$

then for a given constant stress state $\chi(\sigma_{ij})$ we can define a time

$$\overline{t} = \frac{\phi_c V}{\int_V \chi(\sigma_{ij}) dV} \tag{9.18}$$

and eqn. (9.17) becomes

$$\dot{\Psi} = \frac{\phi_c V}{\overline{t}} \tag{9.19}$$

In the present context it can be readily seen that eqns. (9.9) and (9.16) are bounds on $\overline{t}$ for a constant equilibrium stress field σ_{ij}. First consider the bound of eqn. (9.9), then eqn. (9.19) becomes

$$\frac{d\Psi}{dt} \geqslant \int_V \chi(\sigma^s_{ij})\, dV \tag{9.20}$$

where σ^s_{ij} is in equilibrium with the same applied loads as σ_{ij}. If the applied load changes then eqn. (9.20) can be integrated to give

$$\int_0^{\dot{\Psi}_f} d\Psi \geq \int_0^{t_f} \int_V \chi(\sigma^s_{ij})\, dV\, dt \tag{9.21}$$

where t_f is the time to failure and Ψ_f is the value of Ψ at failure, which is less than $\phi_c V$. Therefore eqn. (9.21) becomes

$$\phi_c V \geq \int_0^{t_f} \int_V \chi(\sigma^s_{ij})\, dV\, dt \,. \tag{9.22}$$

If the loading is applied in a cyclic manner with a cycle time of t_c, eqn. (9.22) can be expressed as

$$\phi_c V \geq \bar{t}_f \int_0^1 \int_V \chi(\sigma^s_{ij})\, dV\, d\tau \tag{9.23}$$

where τ is a dimensionless measure of time: $\tau = t/tc$; and $\bar{t}_f$ is the beginning of the cycle at which failure occurs. Rearranging eqn. (9.23) gives

$$\bar{t}_f \leq \frac{\phi_c V}{\int_0^1 \int_V \chi(\sigma^s_{ij})\, dV\, d\tau} \tag{9.24}$$

If the number of cycles to failure is large then $\bar{t}_f$ will be close to t_f.

Similarly, if eqn. (9.16) is used as the bound on $\bar{t}$, we find

$$\bar{t}_f \leq \frac{\phi_c}{\int_0^1 \chi_c\, d\tau} \tag{9.25}$$

where χ_c is a function of τ, and is the value of the yield function that will give plastic collapse at the instantaneous load. Again the bound is retained if χ_c is replaced by $\bar{\chi}_c$, where $\bar{\chi}_c$ corresponds to the yield function which results from an upper bound limit load calculation.

A more interesting, and, perhaps more important, situation is when the

load is cycled fast compared to the characteristic relaxation time for the structure. The above bounds, eqs. (9.24) and (9.25), also apply to this situation, but in certain situations it is possible to obtain better bounds in terms of rapid cycle solutions. As before rapid cycle solutions can be obtained in terms of the deformation solution for a model creeping material or a model plastic material.

Under rapid cycle loading conditions the only variation of stress during a cycle is that due to the elastic response of the material, so that

$$\sigma_{ij}(t) = \hat{\sigma}_{ij}(t) + \rho_{ij} \tag{9.26}$$

where $\hat{\sigma}_{ij}(t)$ is the elastic stress field at a given instant in time and ρ_{ij} is a residual stress field. We assume here that the elastic constants are unaffected by the presence of the damage so that $\sigma_{ij}(t)$ is the same for each cycle. This assumption breaks down when the first element of material fails so that it cannot support any stress. The following are therefore strictly bounds for the time to initiate failure in the components.

9.2.1 Model creeping material

A bound on the life of a component can again be obtained by considering the result of eqn. (9.5). Let σ^2_{ij} of eqn. (9.7) be the actual stress field in the compnent, σ_{ij}, under conditions of rapid cycling and σ^1_{ij} the distribution obtained from the solution for the model creeping material σ^{rc}_{ij}. Integrating eqn. (9.7) over a cycle and then over the volume gives, after noting eqns. (9.6) and (9.26),

$$\int_V (\rho^{rc}_{ij} - \rho_{ij})\, \Delta\varepsilon^p_{ij}\, dV + \int_V \int_0^{t_c} \chi(\sigma_{ij})\, dt\, dV \geq \int_V \int_0^{t_c} \chi(\sigma^{rc}_{ij})\, dt\, dV \tag{9.27}$$

where $\Delta\varepsilon_{ij}^{p} = \int_{o}^{t_c} \dot{\varepsilon}_{ij}^{p}\, dt$ is the compatible inelastic strain accumulated during a cycle of duration t_c. The first term on the l.h.s. of eqn. (9.27) is then identically zero. Substituting eqn. (9.27) into eqn. (9.5) then gives

$$t_f^i = \frac{\phi_c V}{\int_V \int_o^1 \chi(\sigma_{ij}^{rc})\, d\tau\, dV}$$

where, as before, $\tau = t/t_c$.

9.2.2 Model plastic material

Under conditions of rapid cycling shakedown boundary solutions can be used to facilitate the construction of bounds on the time to initiate failure in a component. Ponter [35] considers a general cyclic loading history. Here, however, we limit our attention to the class of problems where the load is cycled between two prescribed limits, Fig. 16. The results can readily be generalized to include the situations considered by Ponter [35].

Again we make use of the inequality of eqn. (9.3) and the convexity condition of eqn. (9.7). As before we identify σ_{ij}^{2} with the actual stress field and σ_{ij}^{1} with the shakedown solution for an elastic perfectly plastic material of yield strength

$$\chi(\sigma_{ij}) = \chi_c \tag{9.29}$$

where the magnitude of χ_c is chosen such that the structure composed of the model plastic material just shakes down. If we now write the associated flow rule in incremental form,

$$d\varepsilon_{ij}^{p} = \mu \frac{\partial \chi(\sigma_{ij})}{\partial \sigma_{ij}}$$

and apply eqn. (9.7) at each extreme of the cycle, we obtain

$$\mu_1 \chi(\sigma_{ij}^1) - \mu_1 \chi(\sigma_{ij}^{1s}) - \mu_1 \frac{\partial \chi(\sigma_{ij}^{1s})}{\partial \sigma_{ij}^{1s}} (\sigma_{ij}^1 - \sigma_{ij}^{1s}) \geq 0$$

(9.30)

$$\mu_2 \chi(\sigma_{ij}^2) - \mu_2 \chi(\sigma_{ij}^{2s}) - \mu_2 \frac{\partial \chi(\sigma_{ij}^{2s})}{\partial \sigma_{ij}^{2s}} (\sigma_{ij}^2 - \sigma_{ij}^{2s}) \geq 0$$

where the first of eqns. (9.30) applied when $0 \leq \tau \leq \lambda$ and the second when $\lambda < \tau \leq 1$. Here we will assume that $\lambda \leq 1 - \lambda$. Combining eqns. (9.30) and noting that plastic straining can only occur when eqn. (9.29) is satisfied leads to the result

$$\frac{\mu_1}{\lambda} \lambda \chi(\sigma_{ij}^1) + \frac{\mu_2}{(1-\lambda)} (1-\lambda) \chi(\sigma_{ij}^2) - (\mu_1 + \mu_2) \chi_c - d\varepsilon_{ij}^p \rho_{ij} \geq 0 \quad (9.31)$$

where $\rho_{ij} = \sigma_{ij}^1 - \sigma_{ij}^{1s} = \sigma_{ij}^2 - \sigma_{ij}^{2s}$ is a residual stress field and $d\varepsilon_{ij}^p$ is the increment of plastic strain experienced by an element of material during a cycle. The inequality of eqn. (9.31) is still retained if μ_1/λ and $\mu_2/(1-\lambda)$ is replaced by $\bar{\mu}$, where $\bar{\mu}$ is the maximum of μ_1/λ and $\mu_2/(1-\lambda)$. Integrating eqn. (9.31) over the volume then gives

$$\int_V \bar{\mu} \{\lambda \chi(\sigma_{ij}^1) + (1-\lambda) \chi(\sigma_{ij}^2)\} dV \geq \chi_c \int_V (\mu_1 + \mu_2) dV \quad (9.32)$$

Multiplying both sides of eqn. (9.3) by $\bar{\mu}$ and integrating over the time to initiate failure and the volume gives

$$t_f^i \int_V \bar{\mu} \{\lambda \chi(\sigma_{ij}^1) + (1-\lambda) \chi(\sigma_{ij}^2)\} dV = \int_V \int_o^{t_f^i} \dot{\phi} \bar{\mu} \, dt dV \quad (9.33)$$

Combining eqns. (9.32) and (9.33) and noting the inequality of eqn. (9.4) gives

$$t_f^i \leq \frac{\phi_c \int_V \overline{\mu}\, dV}{\chi_c \int (\mu_1 + \mu_2) dV} \leq \frac{\phi_c}{\chi_c \lambda} \tag{9.34}$$

The above bound still holds if χ_c is replaced by $\overline{\chi}_c$, the yield function resulting from a kinematic bound for the shakedown solution. As discussed by Ponter [35] this bound can drastically overestimate the time to failure of a component. The eqn. (9.28), (9.24) and (9.25) can then give more accurate estimates of the life.

10. Discussion

The aim of the present paper was to try and obtain a structure for creep constitutive laws through an understanding of the microscopic mechanisms responsible for deformation and failure. This work extends the thermodynamic approach adopted by Rice [1] and Cocks and Ponter [2,3] to include the effects of damage, which exists either in the form of microscopic voids or as dislocation networks whch aid the dislocation climb process. For each mechanism analyzed it is possible to prove the existence of a potential from which the inelastic strain-rate and the damage rate are derivable. This result follows from the fact that the rate of increase of the microscopic damage is driven by its associated thermodynamic force eqn. (2.10). These kinetic relations have been obtained from more detailed analyses of the processes which are responsible for the creeping behavior. For the mechanisms of void growth, the kinetic relations are essentially exact, while for nucleation and the strain-softening mechanism they are semi-empirical in that they are simplifications of the more complex behavior which retain the physics of the process.

The approach adopted here is similar in some respects to that used by [36]. Their measures of damage and their kinetic relationships are however

entirely phenomenological. The structure of their theory is based on the results of Rice [1] for dislocation glide mechanisms of deformation. In this instance the rate of glide of a dislocation is only a function of the thermodynamic force associated with it, so that the resulting potential is only a function of the thermodynamic forces. When considering the various mechanisms of damage we find a slightly different result. Now, the rate of increase of an internal variable which is a measure of the damage is also a function of the present state of damage in the material. The resulting potential is therefore also a function of the present state of damage.

When analyzing the various void growth mechanisms we find that a large number of discrete state variables are required to describe the material response to general loading conditions, section 3. This number can be reduced somewhat by representing the damage in terms of the distribution of cavitated boundaries, section 5. For situations where this distribution of damage is relatively smooth the distribution can be represented by a scalar and a second order tensor state variable. But this is rarely the case and some grain-boundaries generally suffer much more damage than the remainder. There is then a peak in the distribution of damage and higher even order tensors are required to describe the state of the material. If one, however, is only interested certain classes of loading it is possible to identify simple measures of damage that can adequately describe the materials behavior, section 8. For example, in situations where the load is varied in a proportional manner a single scalar measure of damage is sufficient. This damage measure relates to the density of grain-boundary fissures which lie normal, or nearly normal, to the direction of maximum principal stress. When non-proportional loading between two prescribed limits occurs, two scalar state variables are required, which relate to the accumulation of damage

normal to the directions of maximum principal stress at the two extremes.

Over the range of stress and temperature used in the experiments of Leckie and Hayhurst [5,6], and Trampczynski et al [32,33], the results of their tests on copper can be explained in terms of our understanding of the void nucleation and growth mechanisms, section 8. The aluminum alloy tested by them, however, exhibits a completely different type of behavior. They found that even for non-proportional loading histories that a single scalar measure of damage adequately describes the materials response. This is consistent with the analysis of the strain softening mechanism described in section 6.

It is shown in section 9 that when the damage growth rate expression is of the form

$$\dot{\omega} = f(\sigma)\, g(\omega),$$

where ω is a measure of the damage and $f(\sigma)$ and $g(\omega)$ are functions of stress and damage respectively, that it is possible to obtain upper bounds on the life of a component for any loading history. At the present time we are unable to obtain similar results for the more general constitutive relationships obtained in sections 2 through 9.

Acknowledgement

The authors gratefully acknowledge the financial support of the Department of Energy through contract DOE 1198 with the Materials Research Laboratory at the University of Illinois.

References

1. Rice, J. R., "Inelastic Constitutive Relations for Solids: An Internal Variable Theory and its Application to Metal Plasticity," Jnl. Mech. Phys. Solids, 19, 1971, 433.

2. Cocks, A. C. F. and Ponter, A. R. S., "Constitutive Equations for the Plastic Deformation of Solids. I - Isotropic Materials," Leicester University Engineering Department, Report 85-2, 1985.

3. Cocks, A. C. F. and Ponter, A. R. S., "Constitutive Equations for the Plastic Deformation of Solids. II - A Composite Model," Leicester University Engineering Department, Report 85-1, 1985.

4. Ashby, M. F. and Dyson, B. JF., "Creep Damage Mechanics and Micromechanisms," National Physical Laboratory Reprot DMA(A) 77, 1984.

5. Leckie, F. A. and Hayhurst, D. R., "On Creep Rupture in Structures", Proc. Royal Soc., A340, 1974, 324.

6. Leckie, F. A. and Hayhurst, D. R., "Constitutive Equations for Creep Rupture," Acta Met., 25, 1977, 1059.

7. Onat, E. T. and Leckie, F. A., "A Continuum Description of Damage," T&AM Report, No. 469, University of Illinois at Urbana-Champaign, 1984.

8. Henderson, P. J. and McLean, M., "Microstructural Contributions to Friction Stress and Recovery Kinetics During Creep of the Nickel-base Superalloy IN738LC," Acta Met., 31, 1983, 1203.

9. Cocks, A. C. F., "Creep Constitutive Equations for Strain-softening Materials," to appear.

10. Dyson, B. F., "Constrained Cavity Growth, Its Use in Quantifying Recent Creep Fracture Studies," Canad. Met. Quart., 18, 1979, 31.

11. Ponter, A. R. S., Bataille, J., Kestin, J., "A Thermodynamic Model for the Time Dependent Plastic Deformation of Solids," Jnl. de Mec., 18, 1979, 511.

12. Cocks, A. C. F. and Ashby, M. F., "On Creep Fracture by Void Growth," Prog. Mat. Sci., 27, 1982, 189.

13. Duva, J. M., Hutchinson, J. W., "Constitutive Potentials for Dilutely Voided Nonlinear Materials," Division of Applied Sciences, Harvard University, Report MECH-47, 1983.

14. Martin, J. B., "A Note on the Determination of an Upper Bound on Displacement Rates for Steady Creep Problems," Jnl. Applied Mech., 33, 1966, 216.

15. Ponter, A. R. S., "Energy Theorems and Deformation Bounds for Constitutive Relations Associated with Creep and Plastic Deformation of Metals," Jnl. Mech. Phys. Solids, 17, 1969, 493.

16. Cocks, A. C. F., "Creep Deformation of Porous Materials," to appear.

17. Raj, R., Shih, H. M. and Johnson, H. H., "Correction to Intergranular Fracture at Elevated Temperature," Scripta Met., 11, 1977, 839.

18. Chuang, T-J., Kagawa, K. I., Rice, J. R., Sills, L. B., "Non-equilbrium Models for Diffusive Cavitation of Grain Interfaces," Acta Met., 27, 1979, 265.

19. Raj, R. and Ashby, M. F., "Intergranular Fracture at Elevated Temperature," Acta Met., 23, 1975, 653.

20. Argon, A. S., Chen, I-W. and Lau, C-W., "Intergranular Cavitation in Creep: Theory and Experiments," in Cree-Fatigue-Environment Interactions (edited by R. M. Pellouse and N. S. Stoloff), Am. Inst. Min. Engrs., New York, 1980, p 46.

21. Wang, J. S., Stephens, J. J. and Nix, W. D., "A Statistical Analysis of Cavity Nucleation at Particles in Grain Boundaries," Acta Met., 33, 1985, 1009.

22. Cocks, A. C. F., "The Nucleation and Growth of Voids in a Material Containing a Distribution of Grain-boundary Particles," Acta Met., 33, 1985, 129.

23. Hirth, J. P. and Nix, W. D., "Analysis of Cavity Nucleation in Solids Subjected to External and Internal Stresses," Acta Met., 33, 1985, 359.

24. Dyson, B. F., Loveday, M. S. and Rodgers, M. J., "Grain-boundary Cavitation Under Various States of Applied Stress," Proc. Roy. Soc., A349, 1976, 245.

25. Stevens, R. A. and Flewitt, P. E. J., "Dependence of Creep Rate on Microstructure", Acta Met., 29, 1981, 867.

26. Dyson, B. F. and McLean, M., "Particle-Coarsening σ_o and Tertiary Creep," Acta Met., 31, 1983, 17.

27. Shewfelt, R. S. W. and Brown, L. M., "High-temperature Strength of Dispersion-hardened Single Crystals. II Theory," Phil. Mag., 35, 1977, 945.

28. Rice, J. R., "Constraints on the Diffusive Cavitation of Isolated Grain-boundary Facets in Creeping Polycrystals," Acta Met., 31, 1983. 1079.

29. Tvergaard, V., "Constitutive Relations for Creep in Polycrystals, with Grain-boundary Cavitation," Acta Met., 32, 1984, 1977.

30. Tvergaard, V. "Effect of Grain-boundary Sliding on Creep Constrained Diffusive Cavitation," Jnl. Mech. Phys., Solids, 33, 1985, 447.

31. Hutchinson, J. W., "Constitutive Behavior and Crack Tip Fields for Materials Undergoing Creep-constrained Grain-boundary Cavitation," Acta Met., 31, 1983, 1079.

32. Trampczynski, W. A., Hayhurst, D. R. and Leckie, F. A., "Creep Rupture of Copper and Aluminum Under Non-proportional Loading," J. Mech. Phys. Solids, 29, 1981, 353.

33. Hayhurst, D. R., Trampczynski, W. A. and Leckie, F. A., "Creep Rupture Under Non-proportional Loading," Acta Met., 28, 1981, 1171.

34. Cocks, A. C. F. and Leckie, F. A., "Tertiary Creep of Copper," to appear.

35. Ponter, A. R. S., "Upper Bounds on the Creep Rupture Life of Structures Subjected to Variable Load and Temperature," Int. Jnl. Mech. Eng. Sci., 19, 1977, 79.

36. Lemaitre, J. and Chaboche, J. L., "Mécanique des Matériaux Solides" Dunod Paris 1985.

Appendix - Mean strains

In this appendix we obtain expressions for the mean strain experienced by a body when portions of it undergo inelastic deformation. Results are obtained for an anisotropic elastic materials whose stiffness and compliance matrices satisfy the usual symmetry conditions:

$$C_{ijk\ell} = C_{jik\ell} = C_{ij\ell k} = C_{k\ell ij}$$

$$D_{ijk\ell} = D_{jik\ell} = D_{ij\ell k} = D_{k\ell ij} \qquad \text{(A1)}$$

The form and magnitude of these matrices is also allowed to vary with position in the body.

First we consider the situation where a small element of material deforms plastically. Then in section A2 we examine the material's response when discontinuities occur across a plane within the material.

A1 Microscopic inelastic deformation

Consider the situation of Fig. A1 where a volume V' of an element of material of volume V suffers a uniform inelastic strain $d\varepsilon^p_{ij}$. We wish to calculate the mean strain suffered by the larger element. Each strain component must be calculated individually. By way of example we will obtain expressions for the component dE^p_{12}.

Associated with the inelastic strain $d\varepsilon^p_{ij}$ is an elastic strain $d\varepsilon^e_{ij}$, which together form a compatible field, and a residual stress field ρ_{ij}, where

$$\rho_{ij} = C_{ijk\ell}\, d\varepsilon^e_{k\ell} \qquad \text{(A2)}$$

Let $\hat{\sigma}_{ij}$ be the elastic stress distribution in the material for unit applied stresses $\Sigma_{12} = \Sigma_{21}$. Then application of the principle of virtual work gives

$$(dE^p_{12} + dE^p_{21})\ V = 2dE^p_{12}\ V = \int_V \hat{\sigma}_{ij}\ (d\varepsilon^e_{ij} + d\varepsilon^p_{ij})\ dV$$

$$= \int_V C_{ijk\ell}\ \hat{\varepsilon}_{k\ell}(d\varepsilon^e_{ij} + d\varepsilon^p_{ij})\ dV \qquad \text{(A3)}$$

where $\hat{\varepsilon}_{k\ell}$ is the compatible elastic strain field resulting from the application of the unit remote shear stresses. Making use of eqns. (A1) and (A2) the above expression becomes

$$dE^p_{12} = \frac{1}{2V}\left\{\int_V C_{k\ell ij}\ d\varepsilon^e_{ij}\ \hat{\varepsilon}_{k\ell}\ dV + \int_{V^1} \hat{\sigma}_{ij}\ d\varepsilon^p_{ij}\ dV\right\}$$

$$= \frac{1}{2V}\left\{\int_V \rho_{k\ell}\ \hat{\varepsilon}_{k\ell}\ dV + d\varepsilon^p_{ij} \int_{V^1} \hat{\sigma}_{ij}\ dV\right\} \qquad \text{(A4)}$$

The first term on the r.h.s. of eqn. (A4) is zero since ρ_{ij} is a residual stress field and $\hat{\varepsilon}_{k\ell}$ is compatible. Therefore

$$dE^p_{12} = \frac{d\varepsilon^p_{ij}}{2V} \int_{V^1} \hat{\sigma}_{ij}\ dV \qquad \text{(A5)}$$

Similar expressions are readily obtainable for other components of strain. The mean remote strain is related to the local strains through the solution of an elastic problem. For an isotropic elastic material subjected to the stresses $\Sigma_{12} = \Sigma_{21} = 1$, $\hat{\sigma}_{12} = \hat{\sigma}_{21} = 1$, $\hat{\sigma}_{11} = \hat{\sigma}_{22} = \hat{\sigma}_{33} = \hat{\sigma}_{32} = \hat{\sigma}_{23} = 0$, and eqn. (A5) becomes

$$dE^p_{12} = \frac{V^1}{V}\ d\varepsilon^p_{12} \qquad \text{(A6)}$$

or in general

$$dE^p_{ij} = \frac{V^1}{V}\ d\varepsilon^p_{ij} \qquad \text{(A7)}$$

A2 Inelastic stress resulting from internal discontinuous deformations

Consider the body of Fig. A2 which contains a plane of area A with outward normals $\underline{n}^+$ and $\underline{n}^-$. If the positive side of this plane moves an amount $\underline{u}$ w.r.t. the negative side, the body experiences a macroscopic strain dE^p_{ij}. The object of this section is to calculate what these strains are for given internal displacements. Again we do this by considering the equilibrium stress field which results from the application of unit dummy loads in the direction of the required strain. As an example we calculate the shear strains dE^p_{12} and dE^p_{21}. We now treat the body as if it contained an internal surface, S_1 which is subjected to tractions $T^+_i = -\hat{\sigma}_{ij}\, n^+_j$ along S^+_1 and $T^-_i = -\hat{\sigma}_{ij}\, n^-_j$ along S^-_1, where, as before, $\hat{\sigma}_{ij}$ is the elastic stress field resulting from the application of the remote stresses $\Sigma_{12} = \Sigma_{21} = 1$. Application of the principle of virtual work then gives

$$2\, dE^p_{12}\, V + \int_A T^+_i\, u_i\, dS = \int_V \hat{\sigma}_{ij}\, \varepsilon^e_{ij}\, dV \qquad (A8)$$

Making use of eqns. (A1) and (A2) this becomes

$$dE^p_{12} = \frac{1}{2V} \int_A \sigma_{ij}\, n^+_j\, u_i\, dS + \frac{1}{2V} \int_V \rho_{k\ell}\, \hat{\varepsilon}_{k\ell}\, dV \qquad (A9)$$

The second term on the r.h.s. of eqn. (A9) is zero and we have

$$dE^p_{12} = \frac{n_j u_i}{2V} \int_A \hat{\sigma}_{ij}\, dS \qquad (A10)$$

For an isotropic homogeneous material $\hat{\sigma}_{12} = \hat{\sigma}_{21} = 1$ with all other stresses zero and eqn. (A10) becomes

$$dE^p_{12} = \frac{A}{2V} (n_1 u_2 + n_2 u_1)$$

Using the full range of dummy loads we find

$$dE^{p}_{ij} = \frac{A}{2V} (n_i u_j + n_j u_i) \qquad (A11)$$

for an isotropic homogeneous material.

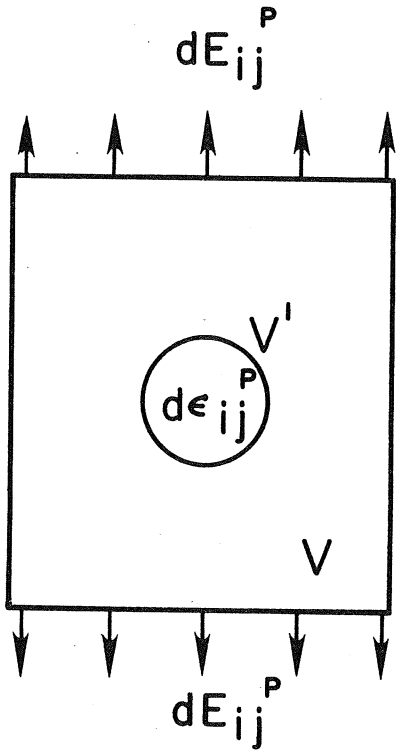

Fig. A1 Macroscopic plastic strain dE_{ij}^P resulting from an increment of plastic strain $d\epsilon_{ij}^P$ in a volume V^1.

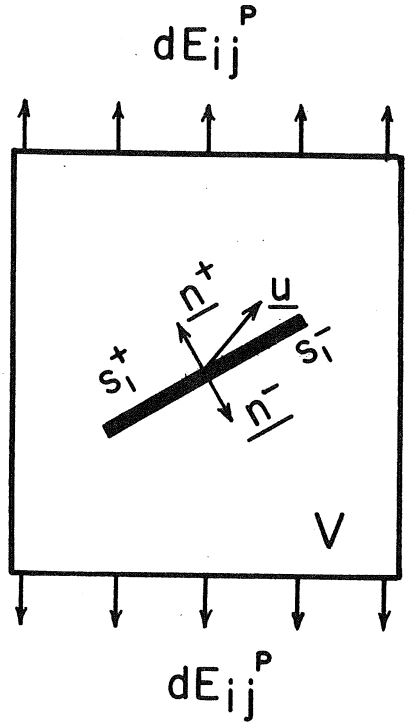

Fig. A2 Macroscopic plastic strain dE_{ij}^P resulting from discontinuous deformation across a plane with outward normals $\underline{n}^+$ and $\underline{n}^-$.

Table 1 - Types of damaging processes identified by Ashby and Dyson [4]

Nucleation and growth of voids	
Coarsening of precipitate particles	Bulk processes
Strain - softening	
Necking	Geometric effect
Oxidation - internal and external	Surface, environment

List of Figures

Fig. A1 Macroscopic plastic strain dE^P_{ij} resulting from an increment of plastic strain $d\varepsilon^p_{ij}$ $d\varepsilon^p_{ij}$ in a volume v^I.

Fig. A2 Macroscopic plastic strain dE^P_{ij} resulting from discontinuous deformation across a plane with outward normals $\underline{n}^+$ and $\underline{n}^-$.